Cardiovascular Computed Tomography in Cardiovascular Disease Diagnosis

Subjects: Radiology, Nuclear Medicine & Medical Imaging | Cardiac & Cardiovascular Systems

Contributor: Zhonghua Sun , Jenna Silberstein , Mauro Vaccarezza

The recent emergence of photon-counting computed tomography (CT) has further enhanced CT performance in clinical applications, providing improved spatial and contrast resolution. CT-derived fractional flow reserve is superior to standard CT-based anatomical assessment for the detection of lesion-specific myocardial ischemia. CT-derived 3D-printed patient-specific models are also superior to standard CT, offering advantages in terms of educational value, surgical planning, and the simulation of cardiovascular disease treatment, as well as enhancing doctor–patient communication. Three-dimensional visualization tools including virtual reality, augmented reality, and mixed reality are further advancing the clinical value of cardiovascular CT in cardiovascular disease.

cardiac computed tomography 3D visualization diagnosis coronary artery disease

1. Introduction

Computed tomography (CT) is a widely used imaging modality in the diagnosis of cardiovascular diseases [1][2][3][4][5][6][7][8][9][10][11][12][13][14]. The diagnostic value of cardiovascular CT has been significantly enhanced with the rapid advancements in CT technologies over the last few decades, allowing for the acquisition of high-resolution images with low radiation doses [15][16][17][18][19]. In addition to the routine use of single-energy CT in daily practice, dual-source and dual-energy CT are becoming increasingly available in most of the current multi-slice CT scanners, further enhancing the diagnostic value of using cardiovascular CT in the context of many cardiovascular diseases [15][16][17][18][19][20][21].

The recent emergence of photon-counting CT (PCCT) represents the latest technological development of CT scanning techniques, with this technique having superior advantages over traditional CT scanners. PCCT enables the acquisition of high-resolution images with improved contrast resolution and simultaneous multi-energy imaging, showing superior advantages over traditional dual-energy CT in cardiovascular imaging [22][23][24][25][26][27][28][29].

Although cardiovascular CT is continuously gaining widespread acceptance and significance, its clinical value mainly focuses more on lumen assessment and the detection of vascular abnormalities, and this feature meets the diagnostic requirements in most situations due to its high diagnostic accuracy, thus serving as the first-line imaging modality in cardiovascular disease [1][2][3][4][5][6][7][8][9][10][11][12][13][14][15][16][17][18][19][20][21]. The well-known limitation of cardiovascular CT lies in the fact that it does not yield functional information, which is more apparent in the assessment of lesion-specific ischemia in coronary artery disease. This has been overcome with the increasing use of CT-derived fractional flow reserve (FFRCT) [30][31][32][33][34]. Single- and multi-center studies have confirmed

that FFRCT can guide patient treatment by identifying lesion-specific ischemia, with coronary CT angiography (CTA) showing improved specificity and positive predictive values when compared to conventional coronary CT angiography (CTA) in the diagnosis of coronary artery disease [35][36][37][38][39][40][41][42][43][44][45][46][47][48].

CT-derived post-processing approaches have transformed the clinical value of cardiovascular CT in cardiovascular disease, and this transformation has led to the creation of patient-specific physical models such as 3D-printed personalized heart and vascular models [49][50][51][52][53][54][55][56][57][58][59][60][61][62][63] and virtual models for visualization, created using virtual reality (VR), augmented reality (AR), and mixed reality (MR) [64][65][66][67][68]. These innovative 3D visualization tools augment the current applications of cardiovascular CT to go beyond the traditional diagnostic approach, as these novel tools can be used for educational purposes, medical training, and the simulation of cardiac procedures, as well as to enhance doctor–patient communication [49][50][51][52][53][54][55][56][57][58][59][60][61][62][63][64][65][66][67][68].

2. Cardiovascular CT: Diagnostic Value Based on Standard Imaging Approach

Cardiovascular CT serves as the first-line imaging modality, being preferred over the gold standard conventional catheter-based angiography in the diagnosis of many cardiovascular diseases, including coronary artery disease (CAD), aortic aneurysms or dissection, peripheral artery disease, and pulmonary embolisms [1][2][3][4][5][6][7][8][9]. This is mainly because of its high diagnostic sensitivity and specificity (>90%) in most of these areas, hence proving that cardiovascular CT is a reliable alternative to conventional angiography. The main driving force of the technological developments in CT lies in cardiac imaging, in particular, the field of coronary CTA in CAD, which comes with strong demands in terms of both spatial resolution to detect and assess small coronary arteries and temporal resolution to allow for the acquisition of cardiac images with few motion-related artifacts [5][6][7][8][9][10]. Recent evidence has highlighted the high sensitivity (>90%) and very high negative predictive value (>98%) of coronary CTA in CAD, indicating that it is a reliable diagnostic tool for determining coronary stenosis. However, it is also a well-known fact that coronary CTA struggles to accurately assess heavily calcified plaques or coronary stented lumens due to blooming artifacts resulting from the extensive calcification and stent wires. This significantly hinders the diagnostic performance of coronary CTA, in particular, compromising its specificity and positive predictive value (PPV), limiting its widespread application in these two particular areas [69][70][71][72][73].

3. Photon-Counting CT: The Latest Technological Advancements in Cardiovascular CT

Photon-counting detectors have the potential to overcome the current CT limitations by directly converting x-ray photons into electric signals, thus optimizing CT dose efficiency at an ultra-high resolution of 0.2 mm. The direct detection of photons also enables photons to be separated into specific energy levels, thus eliminating noise with an improved contrast-to-noise ratio. Further, PCCT allows for the acquisition of multi-energy images simultaneously; hence, PCCT has many benefits in cardiovascular imaging, specifically in assessing calcified

coronary plaques or coronary stents with a reduction in noise and artifacts [21][22]. PCCT was introduced into clinical applications about two years ago, but increasing evidence derived from single- and multi-center studies has demonstrated its superior advantages over the current CT scanners, regardless of the presence of severe calcification in the coronary arteries or coronary stents [23][24][27][74][75][76].

4. Cardiovascular CT: Beyond Lumen Assessment

4.1. Patient-Specific 3D-Printed Models: Medical Education

Three-dimensional printing has become an increasingly useful technology in medical applications, helping to generate patient-specific or personalized models to replicate normal anatomy and pathology with high accuracy. Studies based on randomized controlled trials have provided evidence that confirms the educational value of 3D-printed models in cardiovascular anatomy and pathology when compared to the current teaching methods [63][77][78][79]. The use of 3D-printed models has significantly increased students' knowledge and understanding of complex cardiovascular anatomy and pathology, mainly in congenital heart disease (CHD), compared to the use of diagrams, cadavers, or lectures (the main techniques currently used in teaching) [77][78][79]. However, these randomized controlled studies have some limitations, either due to their small sample sizes, their singular focus on less complex cardiac anatomy without providing insight into the surrounding soft tissue structures [78], or their comparisons of 3D-printed models with virtual visualizations [80][81].

Mogali and colleagues, in a randomized controlled trial, invited first-year medicine students to demonstrate their learning of cardiac anatomy by comparing 3D-printed cardiac models with plastinated cardiac specimens [82]. Three-dimensional printed models were generated by scanning the plastinated cardiac specimens on a 64-slice CT scanner, with the models being printed using multi-color materials (**Figure 1**).

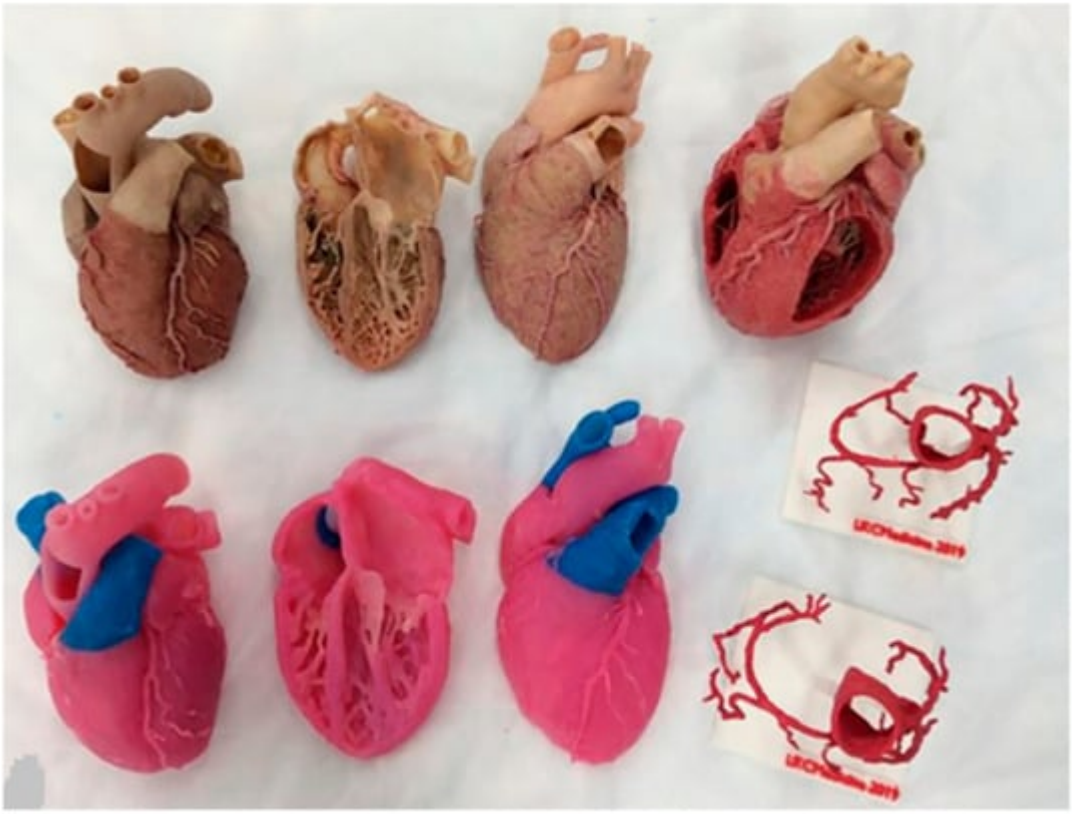

Figure 1. Learning materials provided to the study groups: Phase 1 materials include plastinated cardiac specimens (**top row**) and their three-dimensionally printed replicas and the coronary vessels (**bottom row**). Reprinted with permission from Mogali et al. [82].

Regarding the use of 3D-printed heart and vascular models in anatomy education, the most commonly used imaging modalities are CT or MRI for the generation of 3D-printed models. In a recent study, Arango et al. reported the feasibility of creating ultra-high-resolution 3D-printed heart models using micro-CT [83]. They scanned perfusion-fixed heart specimens using 0.1 mm resolution micro-CT scanning, with the images being post-processed and segmented for 3D printing. The-3D printed heart models accurately represented cardiac walls, vessels, and the valvular and subvalvular structures of atrioventricular valves (**Figure 2** and **Figure 3**), thus serving as useful tools to teach residents and cardiothoracic anesthesia fellows and help them to learn basic and advanced echocardiographic views, valvular pathology, and planned interventions. This study further advances the application of 3D printing technology in cardiovascular anatomy by providing ultra-high-resolution 3D models that demonstrate the finer details of cardiac anatomy.

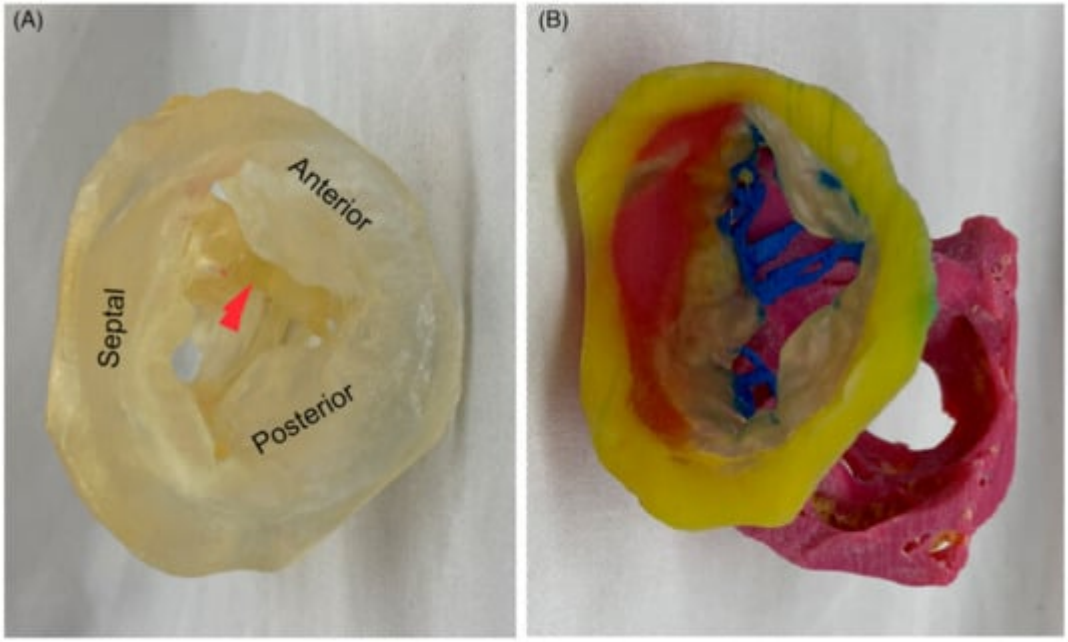

Figure 2. A 3D-printed model of the tricuspid valve of a human heart specimen (HH 223). (**A**) A model printed using a clear material as viewed from the atrium, with leaflets labeled and the moderator band marked with a red arrow. (**B**) A model printed using multiple colors and materials and rotated to show the subvalvular apparatus. Yellow, tricuspid annulus; transparent, mitral leaflets; blue, chordae tendinea; pink, papillary muscles. Reprinted with permission from Arango et al. [83].

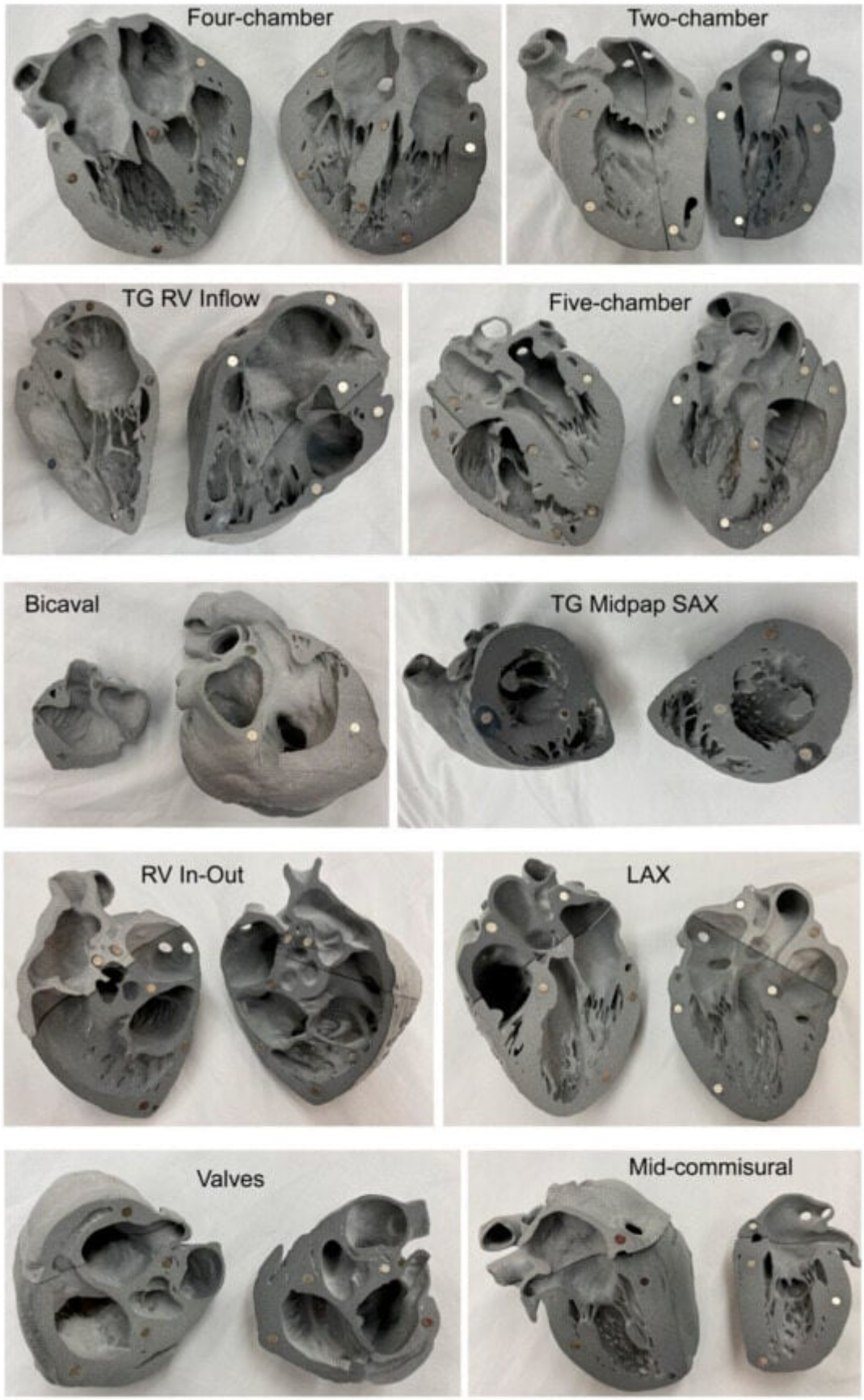

Figure 3. High-resolution fusion powder 3D-printed heart models representing the transesophageal echocardiography (TEE) American Society of Echocardiography (ASE)-recommended views. Each row represents

two corresponding planes on each model that have been labeled accordingly. LAX, long axis; RV, right ventricle; SAX, short axis; TG, transgastric. Reprinted with permission from Arango et al. [83].

4.2. Patient-Specific 3D-Printed Models: Preoperative Planning and Simulation

Three-dimensionally printed personalized models have been shown to play an important role in the planning and simulation of complex cardiovascular procedures, and this has been confirmed by a number of studies based on single-site investigations and multi-center reports [49][50][51][52][53][57][58][59][60][61][62][84][85][86][87][88][89][90][91][92]. Most of the current reports in this area focus on the usefulness of 3D-printed heart models in guiding CHD surgeries. This is most likely due to the complexity and wide variations of CHD, which present challenges for preoperative planning based on traditional 2D and 3D image visualizations. In contrast, 3D-printed personalized models assist cardiac surgeons in planning the treatment of CHD, with up to 50% of surgical decisions involving the aid of 3D-printed models (**Figure 4**) [59].

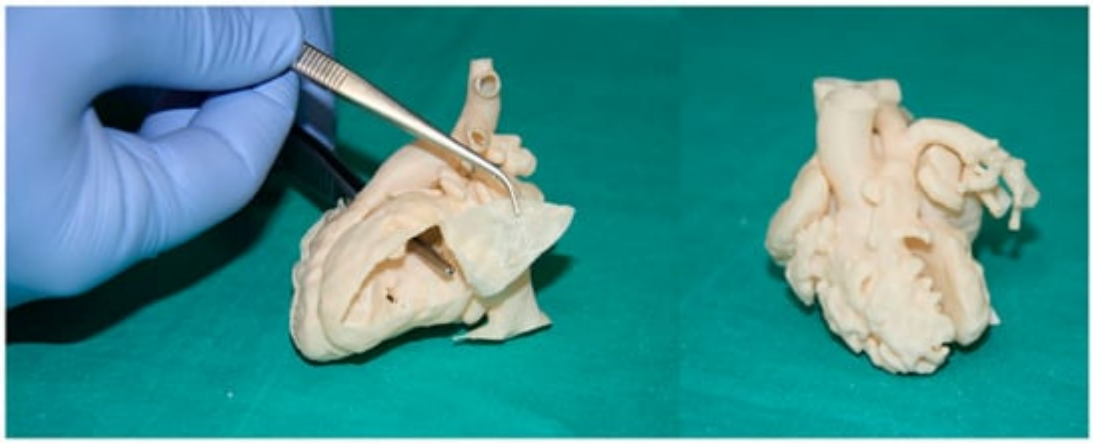

Figure 4. Surgical and interventional planning on 3D-printed heart models. DORV case, internal vision from the left ventricle (**left**). DORV (another case), external view (**right**). DORV-double outlet right ventricle. Reprinted with permission under the open access from Gomez-Ciriza et al. [59].

Three-dimensionally printed models also serve as a useful tool for hands-on surgical training or the simulation of cardiovascular procedures. Three-dimensionally printed heart models can be used to simulate congenital heart surgery with high satisfaction scores. Furthermore, these models are also useful for simulating interventional cardiac procedures such as the simulation of endovascular aortic stent grafting procedures for the treatment of aortic aneurysms or aortic dissection (**Figure 5**) [93]; the simulation of interventional treatment for transcatheter aortic valve replacement (TAVR) for predicting the risk of coronary obstruction or complications [94][95] (**Figure 6**); and simulating valvular stenosis (**Figure 7**) [96]. Another common application of 3D-printed models is their use in guiding left atrial appendage occlude device selection, with improved outcomes and reductions in the number of complications being reported [90][92][97][98][99]. Good agreement in terms of occluder sizes was found between 3D model-based estimation and the actual device sizes, with reduced procedure time and radiation exposure to patients (**Figure 8**) [92].

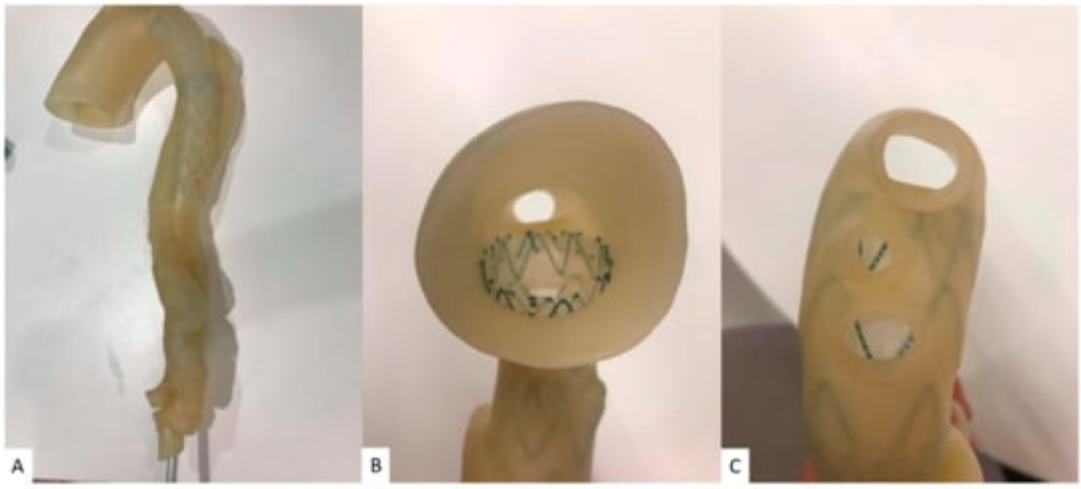

Figure 5. Stent graft deployed in a 3D-printed model. (**A**) Deployed stent graft visible through model wall. (**B**) Axial view from proximal arch. (**C**) Caudal view down arch vessels. Reprinted with permission under open access from Wu et al. [93].

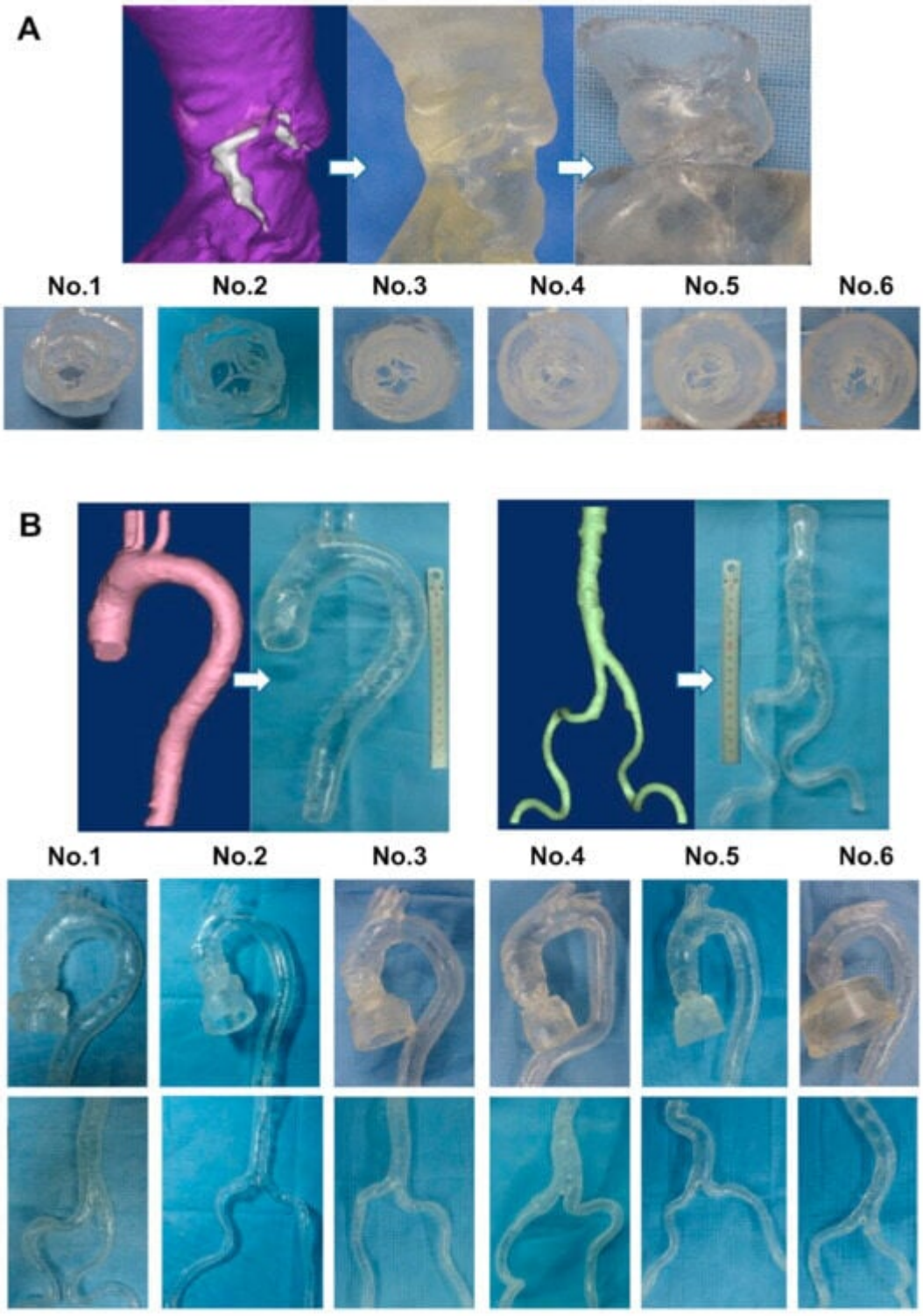
A
No.1
No.2
No.3
No.4
No.5
No.6
B
No.1
No.2
No.3
No.4
No.5
No.6

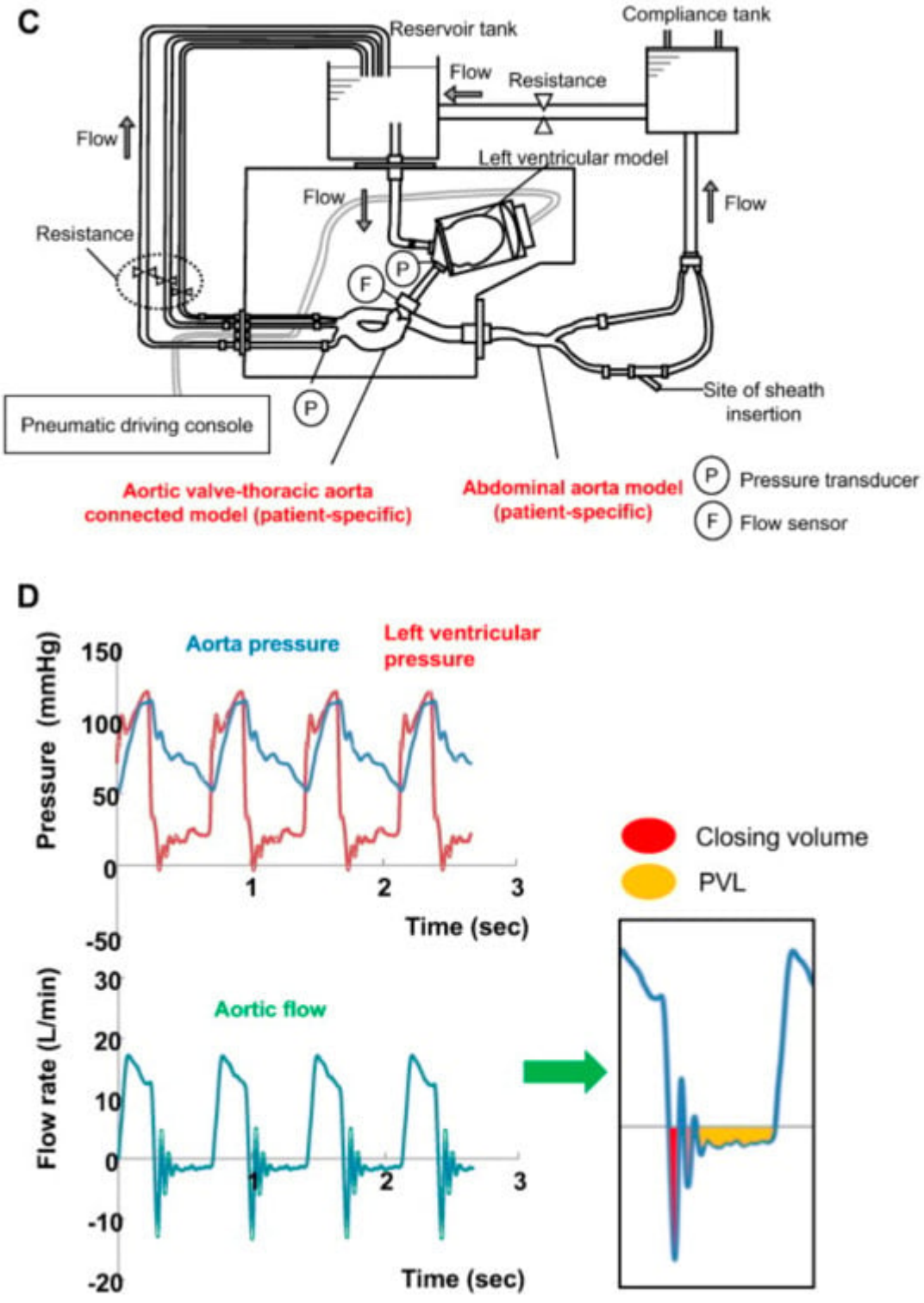

Figure 6. Three-dimensionally printed models with an a pulsatile circulation simulator for the assessment of transcatheter valve hemodynamics. (**A**) Aortic root with left ventricular outflow tract. (**B**) Three-dimensionally printed models of the thoracic aorta, abdominal aorta, and iliofemoral arteries. (**C**) Pulsatile circulation system. (**D**) Representative hemodynamic waveforms of left ventricular pressure (red line), aortic pressure (blue line), flow rate (green line), and the definition of closing volume and PVL (red and yellow areas). PVL = paravalvular leakage. Reprinted with permission from Tanaka et al. [95].

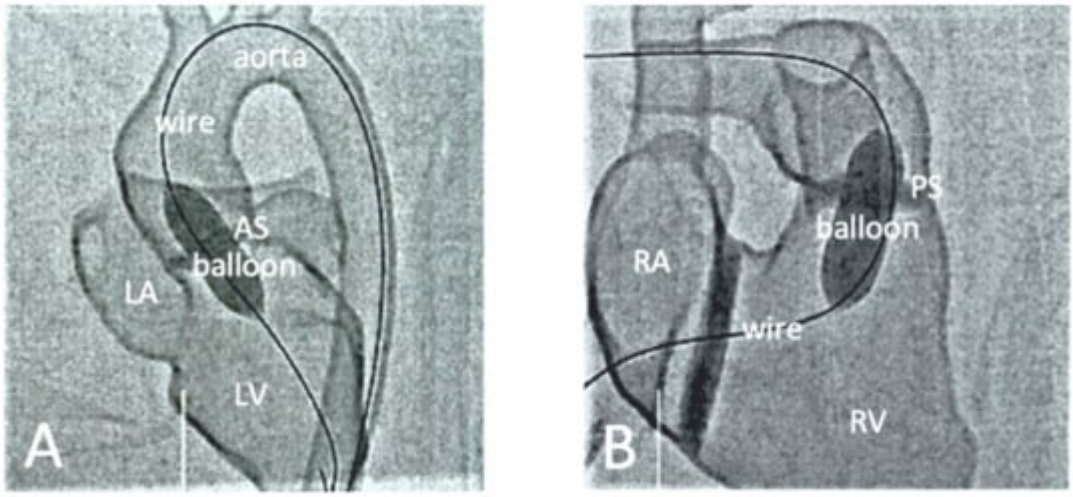

Figure 7. Fluoroscopic documentation of the balloon dilatation of valvular stenoses with a 3D-printed heart model. (**A**) Balloon dilatation of a valvular aortic stenosis. (**B**) Balloon dilatation of a valvular pulmonary stenosis. AS—aortic stenosis, PS—pulmonary stenosis, LA—left atrium, LV—left ventricle, RA—right atrium, RV—right ventricle. Reprinted with permission under the open access from Brunner et al. [96].

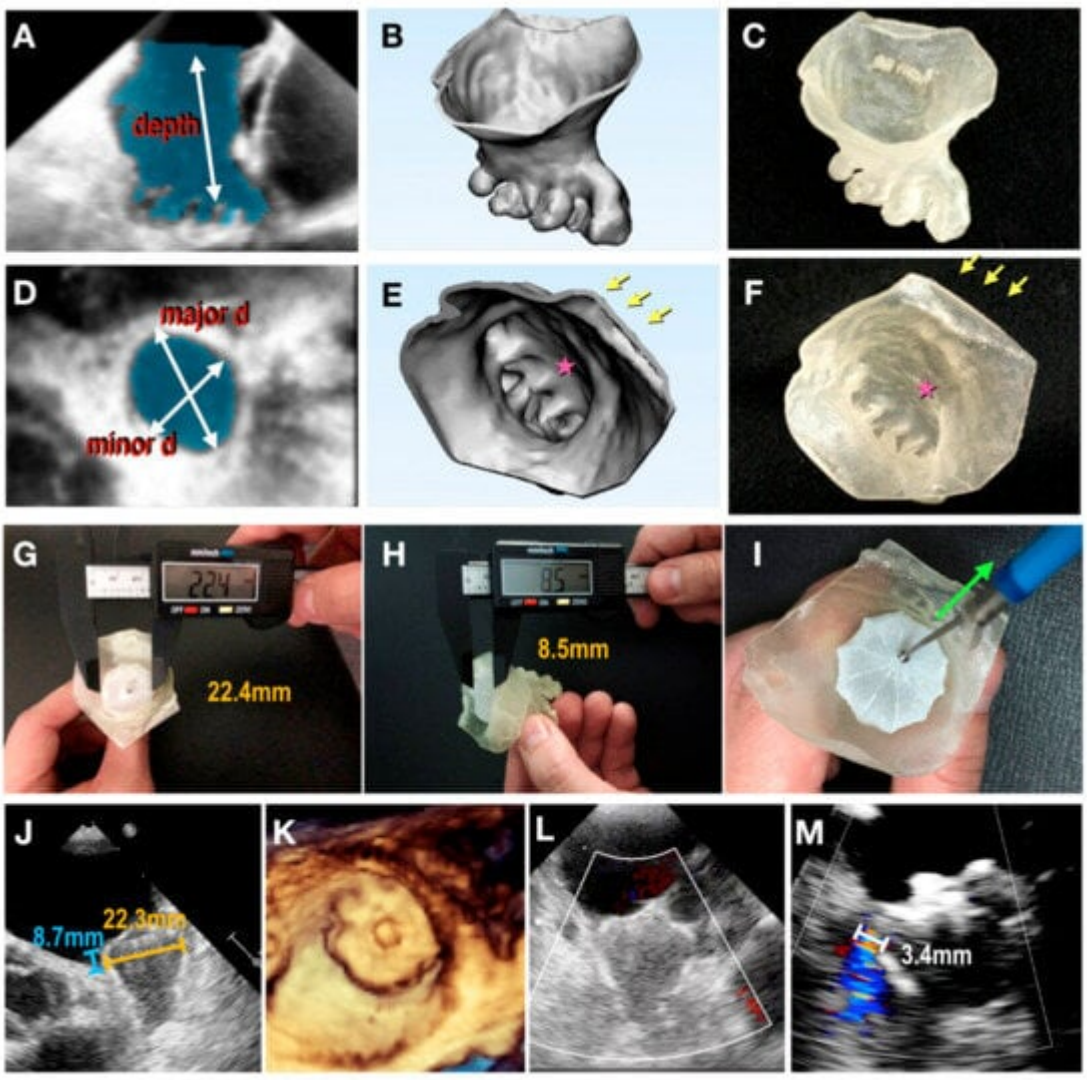

Figure 8. Three-dimensionally printed patient-specific models based on echocardiographic images. (**A**–**F**) From 3D transesophageal echocardiography (TEE) image to 3D physical model. (**A**,**D**) Segmentation of left atrial appendage (LAA) (shaded area) based on 3D TEE data. Measurements regarding the major and minor ostial diameters and depth of the LAA were taken. (**B**,**E**) Creation of a digital object. (**C**,**F**) Three-dimensional printed physical model made of tissue-mimicking material. Arrows denote pulmonary vein ridge; stars denote appendicular trabeculations. (**G**–**I**) Modifying the size of the 3D model. (**G**) Device compression and (**H**) protrusion in 3D model measured using a digital caliper. (**I**) Tug test for stability. (**J**) Device compression and protrusion measured in a clinical procedure. (**K**) Three-dimensional TEE en face view of final device position. (**L**) Color Doppler assessment showing no peridevice leaks. (**M**) In another case, color Doppler assessment revealed a residual leak with a jet width of 3.4 mm. Reprinted with permission under open access from Fan et al. [92].

4.3. Patient-Specific 3D-Printed Models: Clinical Communication

Three-dimensional printed models have enhanced communication between colleagues, clinicians, and patients, as well as the parents of patients. This is clinically important as effective communication contributes to better patient care and clinical outcomes. Physicians usually use visual aids to provide information to patients about their disease/condition and treatment plans or options. However, it can be difficult for patients to comprehend the complexity of cardiovascular anatomy and disease, particularly in more challenging scenarios such as cases of congenital heart disease. The use of physical 3D-printed models overcomes these limitations by presenting a realistic 3D model to the patient so that their understanding of the anatomy and disease is significantly enhanced.

Traynor et al. analyzed 19 studies about the use of 3D printing technology in patient communication [100][101][102][103][104][105][106]. These studies confirmed that 3D-printed models aided communication with patients/parents and colleagues (**Figure 9**) [101].

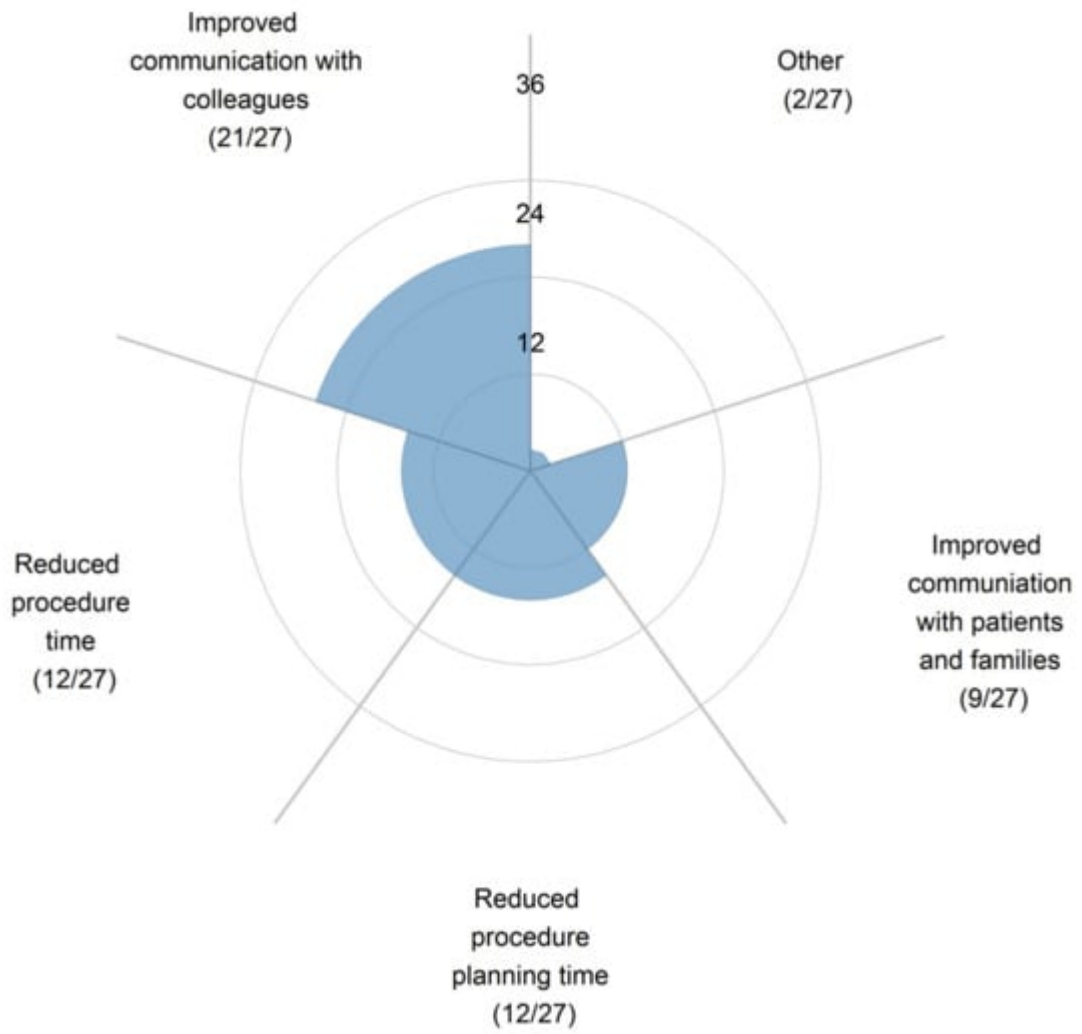

Figure 9. Participants' responses on how 3D-printed cardiac models improve communication with colleagues and patients/families. Reprinted with permission under open access from Illmann et al. [101].

4.4. Patient-Specific 3D-Printed Models: Optimizing CT Protocols

It is well known that CT is associated with relatively high radiation doses; thus, minimizing radiation exposure is clinically significant, given the widespread use of CT in daily practice. The traditional reliance on the use of commercial phantoms to study optimal CT protocols has become less practicable due to expensive costs and the lack of simulations regarding the situations of individual patients. The use of 3D-printed models to optimize cardiovascular CT scanning protocols by representing realistic anatomical structures of cardiovascular systems or organs has become a new research direction [107][108][109][110][111][112][113][114][115].

Sun et al. developed 3D-printed aorta and coronary artery models to study the optimal CT protocols in imaging aortic dissection [113][115] and coronary plaques and stents [108][109][110][116]. Patient-specific coronary artery models were developed to represent realistic coronary artery trees via the simulation of calcified plaques in different locations of coronary arteries showing extensive calcification (**Figure 10**) [108]. This allowed for the study of different CT scanning protocols and the visualization of calcified plaques, which always present challenges in

accurately assessing the degree of coronary stenosis due to the blooming artefacts associated with heavy calcification.

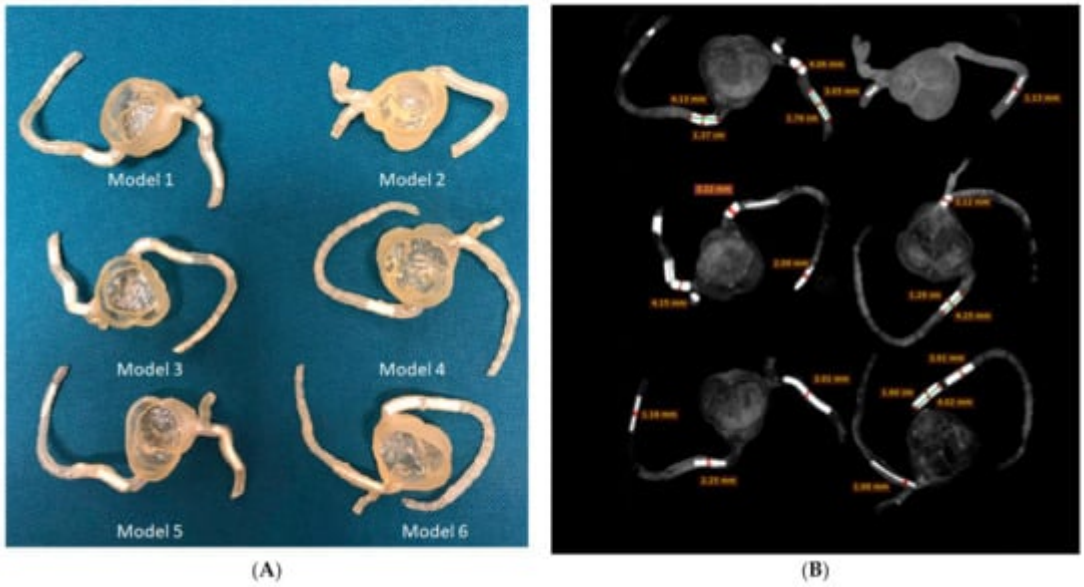

Figure 10. Three-dimensional printed patient-specific coronary models based on the simulation of calcified plaques in the coronary arteries. (**A**) Three-dimensional printed models (*n* = 6) with simulated calcified plaques in coronary artery branches. (**B**) Measurements of plaque dimensions on 2D maximum-intensity projection images using 0.5 mm slice thickness. Reprinted with permission under open access from Sun et al. [108].

4.5. The Use of 3D-Printed Devices in Treating Cardiovascular Disease

Patient-specific 3D-printed devices have been used in treating cardiovascular disease, and promising clinical outcomes have been achieved. It has been reported that 3D-printed devices including stents and valves have improved vessel patency and quality of life in cases of pulmonary stenosis, coronary stenotic lesions, and complex valve pathologies [84][87][90][92][97][98][99][117][118]. The factors that affect the long-term safety of using 3D-printed devices to model stents in patients with coronary artery disease, which include biocompatibility, thrombosis, degradation and mechanical stability, long-term durability and performance, vessel injury, adverse events and complications, patient suitability, and anatomical variability, should be considered [54][119]. Three-dimensional bioprinting is a promising technology advancing the applications of 3D-printed models to another level, although most of the current applications of 3D bioprinting in cardiovascular disease are still in their early stages of development [120]. Significant progress has been achieved over the last decade regarding the use of 3D-printed heart valves in treating valvular heart disease and 3D-printed cardiac patch and heart models in treating myocardial infarction, and heart failure [121][122][123][124][125][126][127][128][129][130][131][132][133][134][135].

4.6. Cardiac CT: CT-Derived FFR

The main limitation of using coronary CTA in predicting the functional significance of coronary stenosis has been addressed using CT-derived fractional flow reserve (FFRCT), and promising clinical outcomes derived from the use

of FFRCT have been achieved in many single-site and multi-center studies.

FFR is the reference method for determining lesion-specific ischemia. The clinical value of FFR-guided patient management strategies has been well studied, with beneficial effects being reported in many studies [66][136][137][138][139][140][141][142][143].

FFRCT has unique advantages over standard coronary CTA by visualizing the coronary stenosis and assessing its hemodynamic significance, thus allowing for a combined anatomic–physiologic assessment of CAD. Representative multi-center studies including DISCOVER-FLOW, NXT, DeFACTO, and NOVEL-FLOW published more than 10 years ago confirmed that FFRCT has an enhanced diagnostic value, as well as especially enhanced specificity in detecting hemodynamically significant CAD when compared to standard coronary CTA based on lumen assessment (**Figure 11**) [41][42][43].

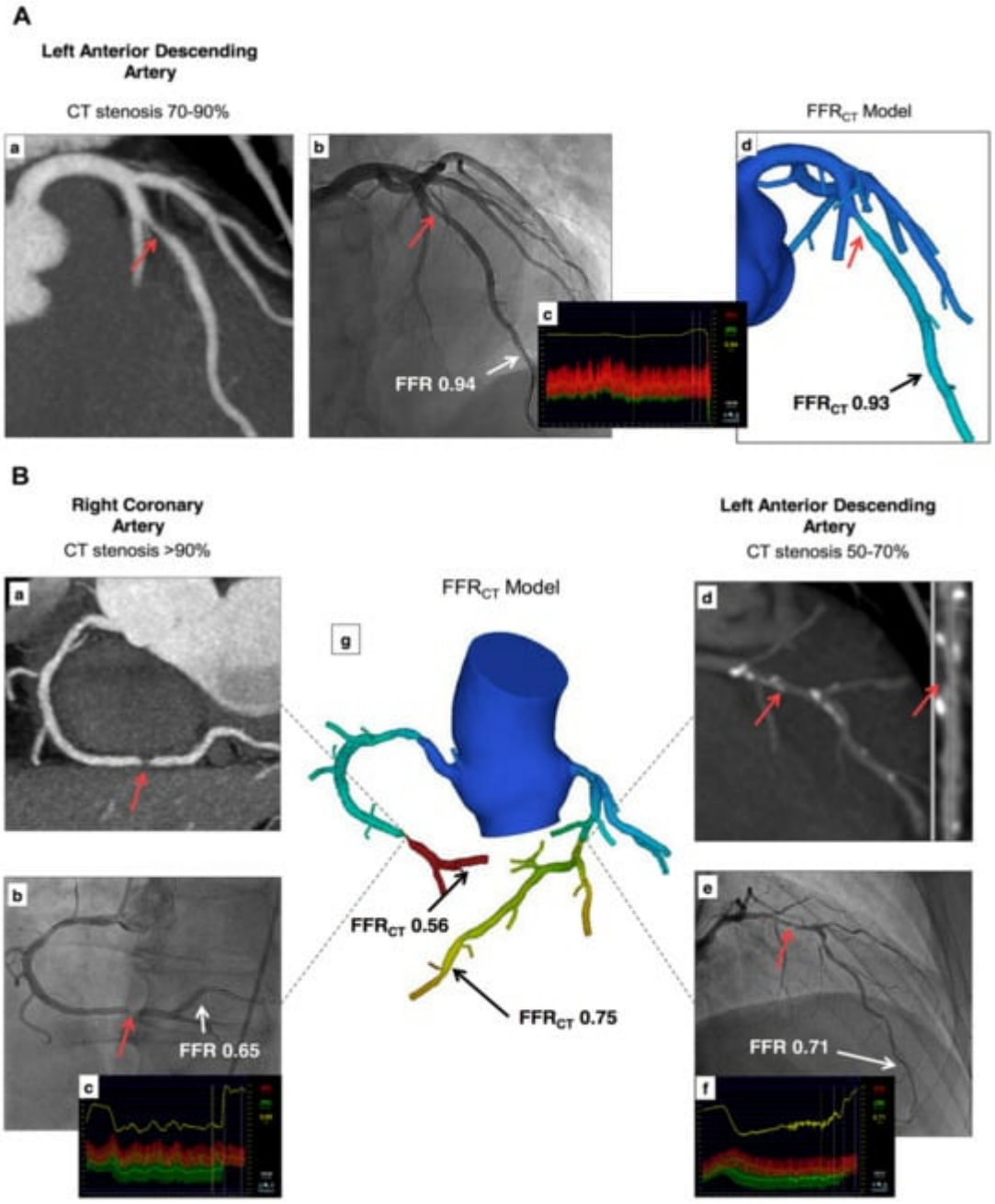

Figure 11. Examples of FFRCT in assessing the hemodynamic significance of coronary lesions at three main coronary arteries (**A**,**B**). Coronary CT angiography shows significant stenoses on the left anterior descending artery (LAD), right coronary artery (RCA), and left circumflex (LCx), while FFRCT shows ischemia at RCA and LCx but not at LAD, as the FFRCT value is more than 0.80. This was confirmed by invasive FFR measurements, as shown in (**A**(**c**)) and (**B**(**c**,**f**)). (**a**,**b**) in image (**A**), (**a**,**b**,**d**,**e**) in image (**B**) refer to stenotic lesions of RCA and LAD on coronary CT angiography and invasive FFR measurements, respectively, while ((**A**)**d**,(**B**)**g**) indicate FFRCT measurements at these coronary arteries. Reprinted with permission from Norgaard et al. [43].

4.7. Cardiovascular CT: VR, AR, and MR

Rapid developments in 3D innovative technologies, including VR, AR, and MR, have further advanced the roles of traditional image visualizations in cardiovascular disease and patient care, with increasing studies proving their educational and clinical value in cardiovascular medicine. Due to complex cardiovascular anatomical and pathological aspects and the importance of lifelong learning and training required to deliver high-quality standards in cardiovascular care, these 3D visualizations serve as useful tools for healthcare providers and patients [64][65][66][67][68][85][144][145][146][147][148][149][150][151][152][153].

VR allows the user to completely immerse themselves in a 3D virtual environment, usually using a head-mounted display (**Figure 12**). In contrast, AR integrates virtual objects into a real-world environment, thus enabling the user to interact with virtual models, improving the simulation and management of complex cardiovascular procedures. MR represents an advancement of AR, and it is a recently developed technology that mainly involves overlaying virtual objects on real world settings (**Figure 13**) [154]. Extended reality (XR) is a new term used to encompass all three of these tools (VR, AR, and MR). The use of VR and AR and MR in medical education and training has been confirmed to improve the understanding of 3D relationships in all medical disciplines [144][145][146][147][148][149][150][151].

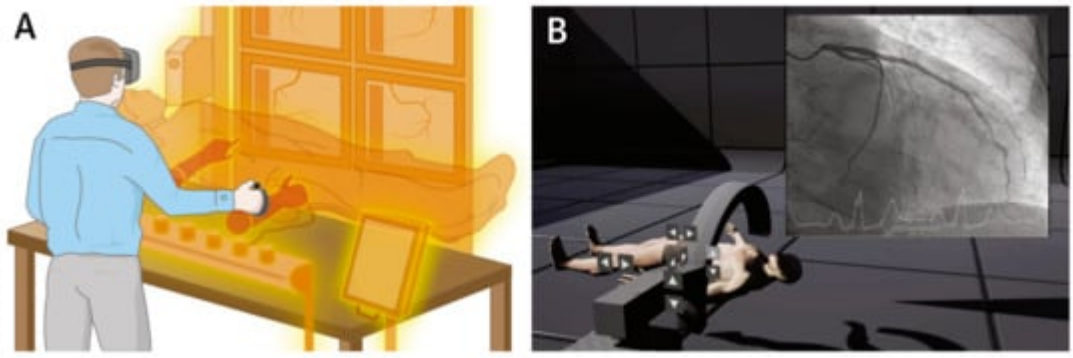

Figure 12. VR completely immersing the user in a virtual 3D space. (**A**) User is completely immersed in a virtual 3D space with use of a head-mounted display. (**B**) A real-life example of VR application allowing trainees to perform virtual coronary angiograms. Reprinted with permission from Jun et al. [144].

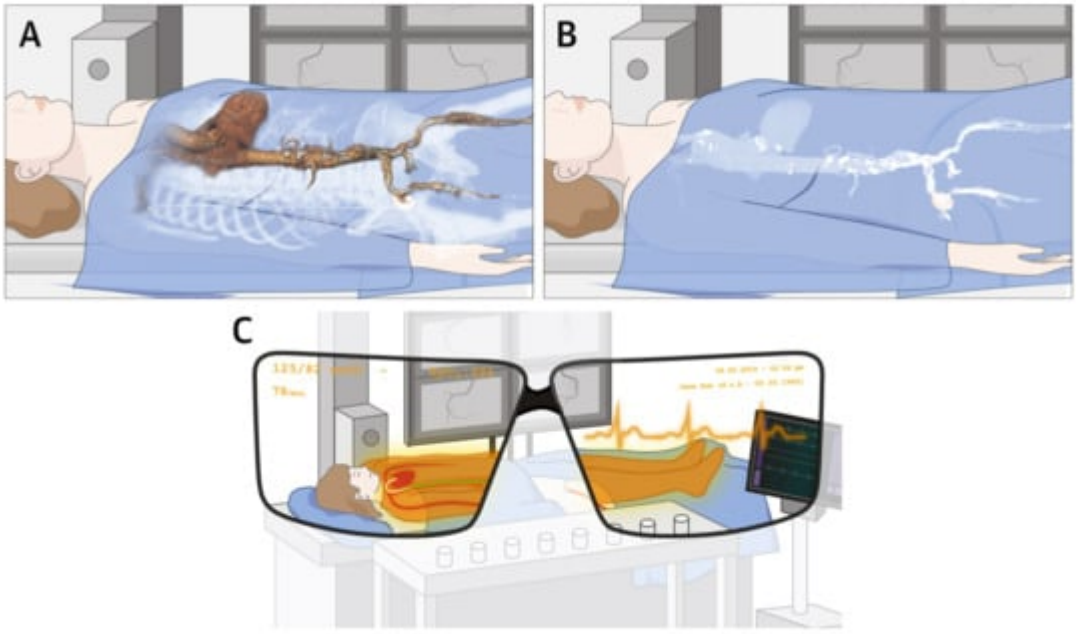

Figure 13. AR integrates superimposed virtual elements into a real-world environment. (**A**) 3D CT image of a patient's vasculature could be imaged by an operator or (**B**) vascular calcifications could be focused to guide the best puncture site and avoid complications during the procedure. (**C**) AR superimposes virtual elements into a real-world environment. Reprinted with permission from Jun et al. [144].

5. Cardiovascular CT: AI/ML/DL

5.1. AI/ML/DL in Coronary Calcium Scoring

Coronary calcium scoring is a routine procedure performed in clinical practice to provide risk stratification for coronary artery disease; however, the quantification of calcium scores could be a time-consuming job, as it still requires the involvement of human observers in interpreting the non-contrast cardiac CT images. AI, specifically DL tools, has been increasingly used for the automated quantification of calcium scores, showing high accuracy compared to manual interpretation [40][155][156][157][158].

5.2. AI/ML/DL in Coronary Artery Disease

The use of advanced AI algorithms has shown significant improvements in assessing calcified plaques, with the results of some studies showing reductions in the number of false-positive rates [159][160][161][162][163]. In a recent study, scholars applied a fine-tuned DL model, the real-enhanced super-resolution generative adversarial network (Real-ESRGAN), to process data pertaining to 50 coronary CTA cases from patients with a total of 184 calcified plaques [159][160]. Measurements of coronary lumen stenosis from AI-processed images were compared to those from original coronary CTA, with ICA being used as the reference method. The Real-ESRGAN -processed images showed improvements in terms of specificity and positive predictive value at all the three main coronary arteries, along with significant reductions in false-positive rates (**Figure 14**).

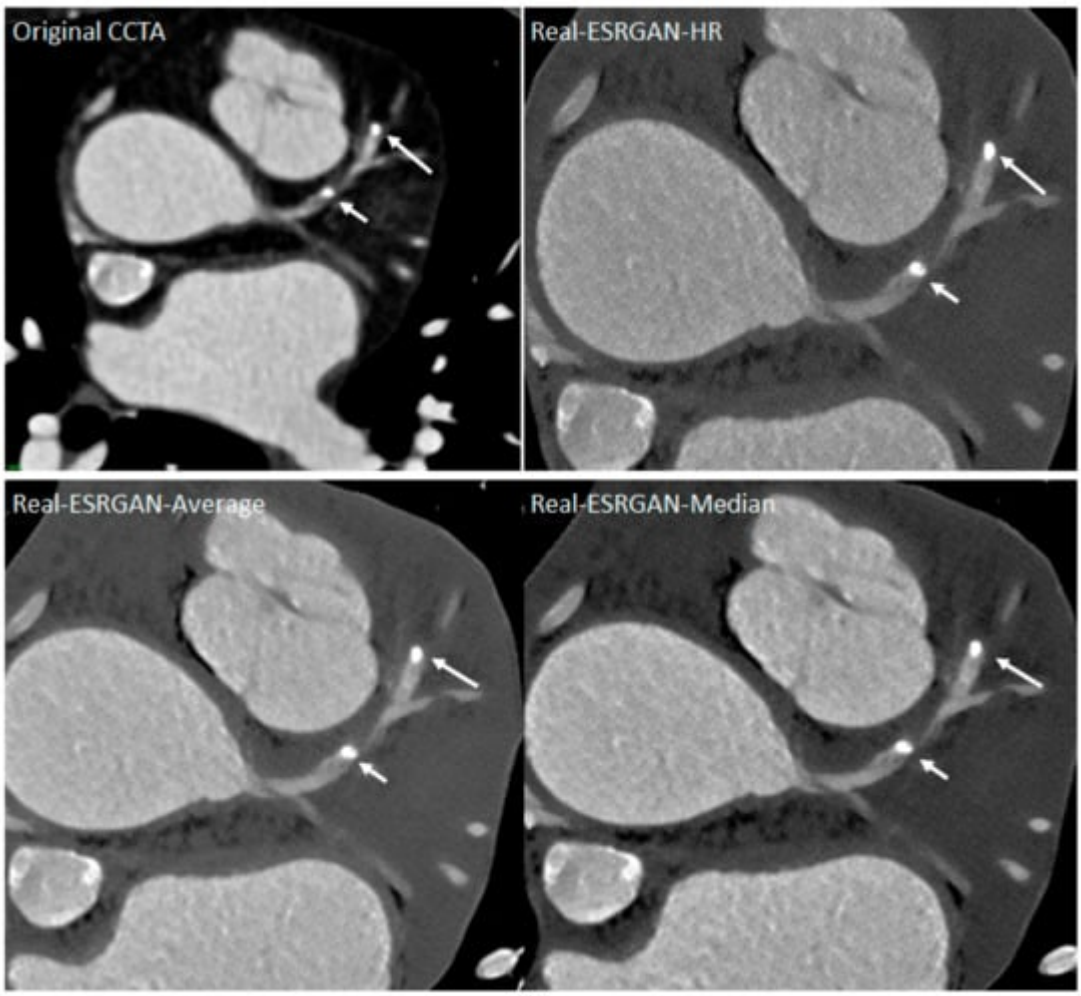
Original CCTA
Real-ESRGAN-HR
Real-ESRGAN-Average
Real-ESRGAN-Median

(A)

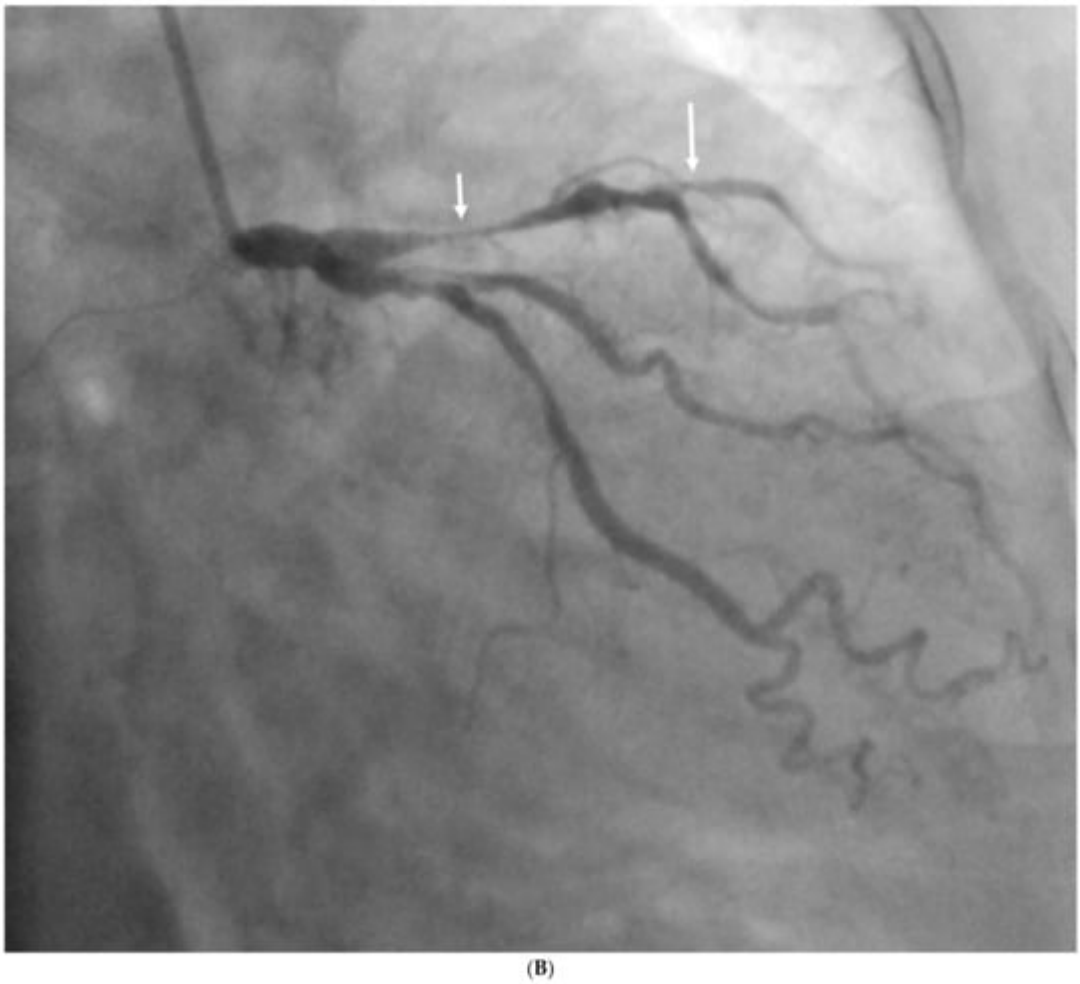

Figure 14. Multiple calcified plaques at the left anterior descending artery (LAD) in a 72-year-old female. Coronary stenoses were measured at 80%, 78%, 72%, and 70% corresponding to the original CCTA, Real-ESRGAN-HR, Real-ESRGAN-Average and Real-ESRGAN-Median images (short arrows in (**A**)), respectively. ICA (short arrow in (**B**)) confirms 75% stenosis. The distal stenoses at LAD due to calcified plaques were measured at 70%, 50%, and 51% stenosis on original CCTA, Real-ESRGAN-HR, and Real-ESRGAN-Average images but measured at 45% on Real-ESRGAN-Median images (long arrows in (**A**)). ICA confirmed the only 37% stenosis (long arrow in (**B**)). CCTA—coronary computed tomography angiography; ESRGAN—enhanced super-resolution generative adversarial network; HR—high resolution; ICA—invasive coronary angiography, Real-ESRGAN—real-enhanced super-resolution generative adversarial network. Reprinted with permission under open access from Sun and Ng [160].

5.3. AI/ML/DL in Abdominal Aortic Aneurysm and Aortic Dissection

Abdominal aortic aneurysm (AAA) is a common and life-threatening cardiovascular disease, and early diagnosis, especially the identification of the aneurysm growth and risk of rupture, plays an important role in improving the management of patients with AAA. The role of AI in the treatment of AAA patients has not been well explored. Raffort et al. conducted a comprehensive review about the usefulness of AI in AAA through an analysis of 34 studies [164]. Of these 34 studies, 15 were related to image segmentation and automation, 14 were related to the

prediction and prognosis of patients, and 5 were related to AAA geometry and fluid dynamic analysis. Manual segmentation is time-consuming and also subject to inter-operator and intra-operator variations. With the use of AI, the mean segmentation time per patient was reduced to 7.4 min as opposed to 25–40 min per patient with the human manual segmentation method (**Figure 15**) [164][165]. This finding is similar to a recent study that showed the feasibility of using AI to screen for AAA [166].

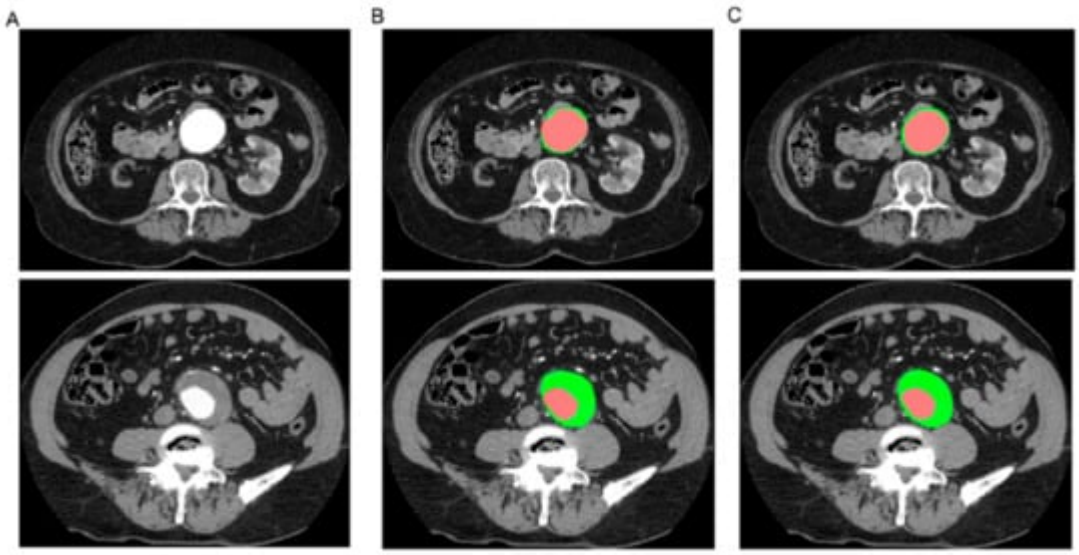

Figure 15. Representative images of the segmentation of the aortic lumen (in red) and the intraluminal thrombus (in green). (**A**) CT scan cross-sectional views of patients with infrarenal AAA. (**B**) Manual segmentation. (**C**) Automatic segmentation. Reprinted with permission under open access from Lareyre et al. [165].

5.4. AI/ML/DL in Pulmonary Artery Disease

CT pulmonary angiography (CTPA) is a standard imaging modality in diagnosing pulmonary embolisms (PEs) with high accuracy. However, the interpretation of CTPA images is time-consuming and requires radiologist expertise. Further, the use of CTPA in emergency departments has increased significantly over the last decades, and increased workloads and fatigue may lead to more diagnostic errors in emergency radiology [167]. Therefore, the use of an automatic PE detection method could assist radiologists' decisions to ensure the rapid diagnosis of positive PE cases while avoiding mistakes.

Studies have reported promising results regarding the application of DL models for the automatic detection of PEs based on CTPA images [168][169][170][171]. A recent systematic review and meta-analysis of using DL in the detection of PEs showed a pooled sensitivity of 88% and a specificity of 86% based on an analysis of five studies [168]. This indicates that further studies are required to validate the DL models to detect PEs based on large datasets of CTPA images. The Radiological Society of North America (RSNA) chose PE as its AI challenge in 2020, later publishing a public dataset of 12,195 annotated CTPA studies to encourage the development of DL models for PE detection [172].

6. Summary

Cardiovascular CT is playing an important role in the diagnosis of cardiovascular disease, and its role will continue to grow with further advancements in CT technology. The traditional reliance on the standard CT imaging approach has been significantly augmented with the use of recent technologies such as photon-counting CT, 3D printing, FFRCT, VR, AR, and MR, and AI. This recent progress has created great opportunities for incorporating these advanced technologies into education and clinical practice to achieve better outcomes.

The clinical value of CT has been further advanced with the recent emergence of photon-counting CT, which can be used to obtain images with superior spatial and contrast resolution. Despite being introduced into clinical practice very recently (in 2021), photon-counting CT represents the future of cardiovascular CT imaging and is set to revolutionize the current cardiovascular CT imaging approach, especially in the diagnostic assessment of cardiovascular disease.

The current applications of 3D printing technology in cardiovascular research are maturing, with more evidence available from multi-center or randomized controlled trials being developed. Three-dimensionally printed models are highly accurate and reliable when it comes to replicating both cardiovascular anatomy and pathology, thus serving as a useful tool for medical education, surgical planning, and the simulation of challenging cardiovascular procedures, guiding intraoperative surgeries to improve patient outcomes. Three-dimensionally printed models improve communication between clinicians and patients, as well as communication between clinical colleagues.

The clinical value of FFRCT has been validated by several multi-center randomized controlled studies and many single-site studies, and its role will continue to grow with the increasing use of DL algorithms in the medical domain. The main barrier to implementing FFRCT in daily cardiology practice lies in the fact that most of the data analyses have been performed at off-site workstations, although on-site image processing and analyses are available, as evidenced by the TARGET trial. With the increasing prevalence of DL models and widespread use of AI in clinical practice, FFRCT will be implemented into diagnostic approaches to guide the revascularization of patients with coronary artery disease, leading to improvements in the utilization of healthcare resources.

VR, AR, and, more recently, MR are showing great promise, and they are set to complement traditional visualizations and assist healthcare providers and patients with cardiovascular disease. However, their applications in current practice are still at an early stage of development due to several limitations. First, the real-time integration of cardiovascular CT imaging in a VR/AR environment is challenging. Second, a critical aspect regarding the use of AR and MR in surgical planning or guiding surgical procedures is to balance AR/MR with the real-world environment and add digital elements to the field of view to achieve the harmonization of data flow and interfaces. Third, ethical considerations need to be considered, as the main goal of using VR/AR/MR should focus on enhancing the patient–provider relationship.

The widespread use of AI in medicine and the application of AI in cardiovascular disease is inevitable, and clinicians must be aware of pitfalls when applying this rapidly evolving technology to their practice. **Figure 16** is a

summary of AI applications in cardiology practice [173]. Given the wide range of AI algorithms available, the input data used for training purposes must be examined to ensure high data quality. AI model performance must be examined to guarantee that findings are robust, and external validation is also an important consideration. Medical graduates and clinicians' skills and confidence in managing AI applications need to be improved, as this will have a direct impact on using AI in clinical practice. Ethical issues related to the sharing of healthcare data and legal challenges should be addressed, and AI should be included in the medical curriculum and professional education. Collaboration among a multi-disciplinary team consisting of computer scientists, clinicians, clinical investigators, academic researchers, and other users is essential for identifying the best approach and data sources to achieve the goal of delivering personalized treatment in cardiovascular disease cases.

Figure 16. The applications of artificial intelligence in clinical cardiology practice. CAC—coronary calcium score, CAD—coronary artery disease, EAT—epicardial adipose tissue, PVAT—perivascular adipose tissue, LV—left ventricle. Reprinted with permission under open access from Jiang et al. [173].

References

1. Gulsin, G.S.; McVeigh, N.; Leipsic, J.A.; Dodd, J.D. Cardiovascular CT and MRI in 2020: Review of key articles. Radiology 2021, 301, 263–277.
2. Sayed, A.; Munir, M.; Bahbah, E.I. Aortic Dissection: A Review of the Pathophysiology, Management and Prospective Advances. Curr. Cardiol. Rev. 2021, 17, e230421186875.
3. Abbas, A.; Brown, I.; Peebles, C.; Harden, S.; Shambrook, J. The role of multidetector-row CT in the diagnosis, classification and management of acute aortic syndrome. Br. J. Radiol. 2014, 87, 20140354.
4. Seitun, S.; Clemente, A.; Maffei, E.; Toia, P.; La Grutta, L.; Cademartiri, F. Prognostic value of cardiac CT. Radiol. Medica 2020, 125, 1135–1147.
5. Sun, Z. Cardiac CT imaging in coronary artery disease: Current status and future directions. Quant. Imaging Med. Surg. 2012, 2, 98–105.
6. Al'Aref, S.J.; Min, J.K. Cardiac CT: Current practice and emerging applications. Heart 2019, 105, 1597–1605.
7. Mayo, J.; Thakur, Y. Pulmonary CT Angiography as First-Line Imaging for PE: Image Quality and Radiation Dose Considerations. AJR Am. J. Roentgenol. 2013, 200, 522–528.
8. Mayo, J.; Thakur, Y. Acute Pulmonary Embolism: From Morphology to Function. Semin. Respir. Crit. Care Med. 2014, 35, 041–049.
9. Corballis, N.; Tsampasian, V.; Merinopoulis, I.; Gunawardena, T.; Bhalraam, U.; Eccleshall, S.; Dweck, M.R.; Vassiliou, V. CT angiography compared to invasive angiography for stable coronary disease as predictors of major adverse cardiovascular events—A systematic review and meta-analysis. Heart Lung 2023, 57, 207–213.
10. Counseller, Q.; Aboelkassem, Y. Recent technologies in cardiac imaging. Front. Med. Technol. 2023, 4, 984492.
11. Newby, D.; Williams, M.; Hunter, A.; Pawade, T.; Shah, A.; Flapan, A.; Forbes, J.; Hargreaves, A.; Stephen, L.; Lewis, S. CT coronary angiography in patients with suspected angina due to coronary heart disease (SCOT-HEART): An open-label, parallel-group, multicentre trial. Lancet 2015, 385, 2383–2391.
12. Maurovich-Horvat, P.; Bosserdt, M.; Kofoed, K.F.; Rieckmann, N.; Benedek, T.; Donnelly, P.; Rodriguez-Palomares, J.; Erglis, A.; Štěchovský, C.; Šakalyte, G. CT or invasive coronary angiography in stable chest pain. N. Engl. J. Med. 2022, 386, 1591–1602.
13. Sun, Z. Diagnostic Accuracy of Multislice CT Angiography in Peripheral Arterial Disease. J. Vasc. Interv. Radiol. 2006, 17, 1915–1921.
14. Walls, M.C.; Thavendiranathan, P.; Rajagopalan, S. Advances in CT angiography for peripheral arterial disease. Cardiol. Clin. 2011, 29, 331–340.

15. Kim, J.W.; Choo, K.S.; Jeon, U.B.; Kim, T.U.; Hwang, J.Y.; Yeom, J.A.; Jeong, H.S.; Choi, Y.Y.; Nam, K.J.; Kim, C.W.; et al. Diagnostic performance and radiation dose of lower extremity CT angiography using a 128-slice dual source CT at 80 kVp and high pitch. Acta. Radiol. 2016, 57, 822–828.
16. Kalisz, K.; Halliburton, S.; Abbara, S.; Leipsic, J.A.; Albrecht, M.H.; Schoepf, U.J.; Rajiah, P. Update on cardiovascular applications of multienergy CT. Radiographics 2017, 37, 1955–1974.
17. Machida, H.; Tanaka, I.; Fukui, R.; Shen, Y.; Ishikawa, T.; Tate, E.; Ueno, E. Dual-energy spectral CT: Various clinical vascular applications. Radiographics 2016, 36, 1215–1232.
18. Litmanovich, D.E.; Tack, D.M.; Shahrzad, M.; Bankier, A.A. Dose reduction in cardiothoracic CT: Review of currently available methods. Radiographics 2014, 34, 1469–1489.
19. Usai, M.V.; Gerwing, M.; Gottschalk, A.; Sporns, P.; Heindel, W.; Oberhuber, A.; Wildgruber, M.; Köhler, M. Intra-arterial catheter-directed CT angiography for assessment of endovascular aortic aneurysm repair. PLoS ONE 2019, 14, e0221375.
20. Schuijf, J.D.; Lima, J.A.C.; Boedeker, K.L.; Takagi, H.; Tanaka, R.; Yoshioka, K.; Arbab-Zadeh, A. CT imaging with ultra-high-resolution: Opportunities for cardiovascular imaging in clinical practice. J. Cardiovasc. Comput. Tomogr. 2022, 16, 388–396.
21. Tortora, M.; Gemini, L.; D'Iglio, I.; Ugga, L.; Spadarella, G.; Cuocolo, R. Spectral Photon-Counting Computed Tomography: A Review on Technical Principles and Clinical Applications. J. Imaging 2022, 8, 112.
22. Cademartiri, F.; Meloni, A.; Pistoia, L.; Degiorgi, G.; Clemente, A.; Gori, C.D.; Positano, V.; Celi, S.; Berti, S.; Emdin, M.; et al. Dual-Source Photon-Counting Computed Tomography— Part I: Clinical Overview of Cardiac CT and Coronary CT Angiography Applications. J. Clin. Med. 2023, 12, 3627.
23. Si-Mohamed, S.A.; Boccalini, S.; Lacombe, H.; Diaw, A.; Varasteh, M.; Rodesch, P.-A.; Dessouky, R.; Villien, M.; Tatard-Leitman, V.; Bochaton, T. Coronary CT angiography with photon-counting CT: First-in-human results. Radiology 2022, 303, 303–313.
24. Flohr, T.; Schmidt, B.; Ulzheimer, S.; Alkadhi, H. Cardiac imaging with photon counting CT. Br. J. Radiol. 2023, 96, 20230407.
25. Allmendinger, T.; Nowak, T.; Flohr, T.; Klotz, E.; Hagenauer, J.; Alkadhi, H.; Schmidt, B. Photon-Counting Detector CT-Based Vascular Calcium Removal Algorithm: Assessment Using a Cardiac Motion Phantom. Investig. Radiol. 2022, 57, 399–405.
26. Boccalini, S.; Si-Mohamed, S.A.; Lacombe, H.; Diaw, A.; Varasteh, M.; Rodesch, P.A.; Villien, M.; Sigovan, M.; Dessouky, R.; Coulon, P.; et al. First in-Human Results of Computed Tomography Angiography for Coronary Stent Assessment with a Spectral Photon Counting Computed Tomography. Investig. Radiol. 2022, 57, 212–221.

27. Koons, E.; VanMeter, P.; Rajendran, K.; Yu, L.; McCollough, C.; Leng, S. Improved quantification of coronary artery luminal stenosis in the presence of heavy calcifications using photon-counting detector CT. Proc. SPIE. Int. Soc. Opt. Eng. 2022, 12031, 120311A.

28. Meloni, A.; Frijia, F.; Panetta, D.; Degiorgi, G.; De Gori, C.; Maffei, E.; Clemente, A.; Positano, V.; Cademartiri, F. Photon-counting computed tomography (pcct): Technical background and cardiovascular applications. Diagnostics 2023, 13, 645.

29. Bech, G.J.W.; De Bruyne, B.; Pijls, N.H.; De Muinck, E.D.; Hoorntje, J.C.; Escaned, J.; Stella, P.R.; Boersma, E.; Bartunek, J.; Koolen, J.J. Fractional flow reserve to determine the appropriateness of angioplasty in moderate coronary stenosis: A randomized trial. Circulation 2001, 103, 2928–2934.

30. Tavoosi, A.; Kadoya, Y.; Chong, A.Y.; Small, G.R.; Chow, B.J.W. Utility of FFRCT in Patients with Chest Pain. Curr. Atheroscler. Rep. 2023, 25, 427–434.

31. Chen, J.; Wetzel, L.H.; Pope, K.L.; Meek, L.J.; Rosamond, T.; Walker, C.M. FFRCT: Current Status. AJR Am. J. Roentgenol. 2020, 216, 640–648.

32. Ihdayhid, A.R.; Norgaard, B.L.; Gaur, S.; Leipsic, J.; Nerlekar, N.; Osawa, K.; Miyoshi, T.; Jensen, J.M.; Kimura, T.; Shiomi, H. Prognostic value and risk continuum of noninvasive fractional flow reserve derived from coronary CT angiography. Radiology 2019, 292, 343–351.

33. Kawaji, T.; Shiomi, H.; Morishita, H.; Morimoto, T.; Taylor, C.A.; Kanao, S.; Koizumi, K.; Kozawa, S.; Morihiro, K.; Watanabe, H.; et al. Feasibility and diagnostic performance of fractional flow reserve measurement derived from coronary computed tomography angiography in real clinical practice. Int. J. Cardiovasc. Imaging 2017, 33, 271–281.

34. Nørgaard, B.L.; Jensen, J.M.; Blanke, P.; Sand, N.P.; Rabbat, M.; Leipsic, J. Coronary CT Angiography Derived Fractional Flow Reserve: The Game Changer in Noninvasive Testing. Curr. Cardiol. Rep. 2017, 19, 112.

35. Xu, L.; Sun, Z.; Fan, Z. Noninvasive Physiologic Assessment of Coronary Stenoses Using Cardiac CT. BioMed Res. Int. 2015, 2015, 435737.

36. Gao, X.; Wang, R.; Sun, Z.; Zhang, H.; Bo, K.; Xue, X.; Yang, J.; Xu, L. A Novel CT Perfusion-Based Fractional Flow Reserve Algorithm for Detecting Coronary Artery Disease. J. Clin. Med. 2023, 12, 2154.

37. Fairbairn, T.A.; Nieman, K.; Akasaka, T.; Nørgaard, B.L.; Berman, D.S.; Raff, G.; Hurwitz-Koweek, L.M.; Pontone, G.; Kawasaki, T.; Sand, N.P.; et al. Real-world clinical utility and impact on clinical decision-making of coronary computed tomography angiography-derived fractional flow reserve: Lessons from the ADVANCE Registry. Eur. Heart J. 2018, 39, 3701–3711.

38. Xue, X.; Liu, X.; Gao, Z.; Wang, R.; Xu, L.; Ghista, D.; Zhang, H. Personalized coronary blood flow model based on CT perfusion to non-invasively calculate fractional flow reserve. Comput.

Methods Appl. Mech. Eng. 2023, 404, 115789.

39. Donnelly, P.M.; Kolossváry, M.; Karády, J.; Ball, P.A.; Kelly, S.; Fitzsimons, D.; Spence, M.S.; Celeng, C.; Horváth, T.; Szilveszter, B.; et al. Experience with an on-Site Coronary Computed Tomography-Derived Fractional Flow Reserve Algorithm for the Assessment of Intermediate Coronary Stenoses. Am. J. Cardiol. 2018, 121, 9–13.
40. Yang, D.H.; Kim, Y.-H.; Roh, J.H.; Kang, J.-W.; Ahn, J.-M.; Kweon, J.; Lee, J.B.; Choi, S.H.; Shin, E.-S.; Park, D.-W.; et al. Diagnostic performance of on-site CT-derived fractional flow reserve versus CT perfusion. Eur. Heart J.—Cardiovasc. Imaging 2016, 18, 432–440.
41. Koo, B.-K.; Erglis, A.; Doh, J.-H.; David, V.D.; Jegere, S.; Kim, H.-S.; Dunning, A.; DeFrance, T.; Lansky, A.; Leipsic, J.; et al. Diagnosis of Ischemia-Causing Coronary Stenoses by Noninvasive Fractional Flow Reserve Computed from Coronary Computed Tomographic Angiograms. J. Am. Coll. Cardiol. 2011, 58, 1989–1997.
42. Yoon, Y.E.; Choi, J.-H.; Kim, J.-H.; Park, K.-W.; Doh, J.-H.; Kim, Y.-J.; Koo, B.-K.; Min, J.K.; Erglis, A.; Gwon, H.-C.; et al. Noninvasive Diagnosis of Ischemia-Causing Coronary Stenosis Using CT Angiography. JACC Cardiovasc. Imaging 2012, 5, 1088–1096.
43. Nørgaard, B.L.; Leipsic, J.; Gaur, S.; Seneviratne, S.; Ko, B.S.; Ito, H.; Jensen, J.M.; Mauri, L.; De Bruyne, B.; Bezerra, H.; et al. Diagnostic Performance of Noninvasive Fractional Flow Reserve Derived from Coronary Computed Tomography Angiography in Suspected Coronary Artery Disease. J. Am. Coll. Cardiol. 2014, 63, 1145–1155.
44. Colleran, R.; Douglas, P.S.; Hadamitzky, M.; Gutberlet, M.; Lehmkuhl, L.; Foldyna, B.; Woinke, M.; Hink, U.; Nadjiri, J.; Wilk, A. An FFRCT diagnostic strategy versus usual care in patients with suspected coronary artery disease planned for invasive coronary angiography at German sites: One-year results of a subgroup analysis of the PLATFORM (Prospective Longitudinal Trial of FFRCT: Outcome and Resource Impacts) study. Open Heart 2017, 4, e000526.
45. Douglas, P.S.; Pontone, G.; Hlatky, M.A.; Patel, M.R.; Norgaard, B.L.; Byrne, R.A.; Curzen, N.; Purcell, I.; Gutberlet, M.; Rioufol, G.; et al. Clinical outcomes of fractional flow reserve by computed tomographic angiography-guided diagnostic strategies vs. usual care in patients with suspected coronary artery disease: The prospective longitudinal trial of FFRCT: Outcome and resource impacts study. Eur. Heart J. 2015, 36, 3359–3367.
46. Patel, M.R.; Nørgaard, B.L.; Fairbairn, T.A.; Nieman, K.; Akasaka, T.; Berman, D.S.; Raff, G.L.; Koweek, L.M.H.; Pontone, G.; Kawasaki, T.; et al. 1-Year Impact on Medical Practice and Clinical Outcomes of FFRCT. JACC Cardiovasc. Imaging 2020, 13, 97–105.
47. Curzen, N.P.; Nolan, J.; Zaman, A.G.; Nørgaard, B.L.; Rajani, R. Does the Routine Availability of CT–Derived FFR Influence Management of Patients with Stable Chest Pain Compared to CT Angiography Alone?: The FFRCT RIPCORD Study. JACC Cardiovasc. Imaging 2016, 9, 1188–1194.

48. Curzen, N.; Nicholas, Z.; Stuart, B.; Wilding, S.; Hill, K.; Shambrook, J.; Eminton, Z.; Ball, D.; Barrett, C.; Johnson, L.; et al. Fractional flow reserve derived from computed tomography coronary angiography in the assessment and management of stable chest pain: The FORECAST randomized trial. Eur. Heart J. 2021, 42, 3844–3852.
49. Giannopoulos, A.A.; Steigner, M.L.; George, E.; Barile, M.; Hunsaker, A.R.; Rybicki, F.J.; Mitsouras, D. Cardiothoracic Applications of 3-dimensional Printing. J. Thorac. Imaging 2016, 31, 253–272.
50. Costello, J.P.; Olivieri, L.J.; Krieger, A.; Thabit, O.; Marshall, M.B.; Yoo, S.-J.; Kim, P.C.; Jonas, R.A.; Nath, D.S. Utilizing Three-Dimensional Printing Technology to Assess the Feasibility of High-Fidelity Synthetic Ventricular Septal Defect Models for Simulation in Medical Education. World. J. Pediatr. Congenit. Heart Surg. 2014, 5, 421–426.
51. Costello, J.P.; Olivieri, L.J.; Su, L.; Krieger, A.; Alfares, F.; Thabit, O.; Marshall, M.B.; Yoo, S.J.; Kim, P.C.; Jonas, R.A. Incorporating three-dimensional printing into a simulation-based congenital heart disease and critical care training curriculum for resident physicians. Congenit. Heart Dis. 2015, 10, 185–190.
52. Sun, Z.; Lau, I.; Wong, Y.H.; Yeong, C.H. Personalized three-dimensional printed models in congenital heart disease. J. Clin. Med. 2019, 8, 522.
53. Sun, Z.; Shen-Yuan, L. A systematic review of 3-D printing in cardiovascular and cerebrovascular diseases. Anatol. J. Cardiol. 2017, 17, 423–435.
54. Shabbak, A.; Masoumkhani, F.; Fallah, A.; Amani-Beni, R.; Mohammadpour, H.; Shahbazi, T.; Bakhshi, A. 3D printing for cardiovascular surgery and intervention: A review article. Curr. Probl. Cardiol. 2024, 49, 102086.
55. Lau, I.; Sun, Z. Three-dimensional printing in congenital heart disease: A systematic review. J. Med. Radiat. Sci. 2018, 65, 226–236.
56. Verghi, E.; Catanese, V.; Nenna, A.; Montelione, N.; Mastroianni, C.; Lusini, M.; Stilo, F.; Chello, M. 3D printing in cardiovascular disease: Current appplications an future perspectives. Surg. Technol. Int. 2021, 38, 314–324.
57. Lau, I.W.W.; Sun, Z. Dimensional Accuracy and Clinical Value of 3D Printed Models in Congenital Heart Disease: A Systematic Review and Meta-Analysis. J. Clin. Med. 2019, 8, 1483.
58. Sun, Z. Clinical Applications of Patient-Specific 3D Printed Models in Cardiovascular Disease: Current Status and Future Directions. Biomolecules 2020, 10, 1577.
59. Gómez-Ciriza, G.; Gómez-Cía, T.; Rivas-González, J.A.; Forte, M.N.V.; Valverde, I. Affordable three-dimensional printed heart models. Front. Cardiovasc. Med. 2021, 8, 642011.

60. Moore, R.A.; Riggs, K.W.; Kourtidou, S.; Schneider, K.; Szugye, N.; Troja, W.; D'Souza, G.; Rattan, M.; Bryant, R., III; Taylor, M.D. Three-dimensional printing and virtual surgery for congenital heart procedural planning. Birth Defects Res. 2018, 110, 1082–1090.
61. Garas, M.; Vaccarezza, M.; Newland, G.; McVay-Doornbusch, K.; Hasani, J. 3D-Printed specimens as a valuable tool in anatomy education: A pilot study. Ann. Anat. 2018, 219, 57–64.
62. Anwar, S.; Rockefeller, T.; Raptis, D.A.; Woodard, P.K.; Eghtesady, P. 3D Printing Provides a Precise Approach in the Treatment of Tetralogy of Fallot, Pulmonary Atresia with Major Aortopulmonary Collateral Arteries. Curr. Treat. Options Cardiovasc. Med. 2018, 20, 5.
63. Loke, Y.-H.; Harahsheh, A.S.; Krieger, A.; Olivieri, L.J. Usage of 3D models of tetralogy of Fallot for medical education: Impact on learning congenital heart disease. BMC Med. Educ. 2017, 17, 54.
64. Bouraghi, H.; Mohammadpour, A.; Khodaveisi, T.; Ghazisaeedi, M.; Saeedi, S.; Familgarosian, S. Virtual Reality and Cardiac Diseases: A Systematic Review of Applications and Effects. J. Healthc. Eng. 2023, 2023, 8171057.
65. Stephenson, N.; Pushparajah, K.; Wheeler, G.; Deng, S.; Schnabel, J.A.; Simpson, J.M. Extended reality for procedural planning and guidance in structural heart disease—A review of the state-of-the-art. Int. J. Cardiovasc. Imaging 2023, 39, 1405–1419.
66. Maresky, H.; Oikonomou, A.; Ali, I.; Ditkofsky, N.; Pakkal, M.; Ballyk, B. Virtual reality and cardiac anatomy: Exploring immersive three-dimensional cardiac imaging, a pilot study in undergraduate medical anatomy education. Clin. Anat. 2019, 32, 238–243.
67. Barteit, S.; Lanfermann, L.; Bärnighausen, T.; Neuhann, F.; Beiersmann, C. Augmented, mixed, and virtual reality-based head-mounted devices for medical education: Systematic review. JMIR Serious Games 2021, 9, e29080.
68. Dhar, P.; Rocks, T.; Samarasinghe, R.M.; Stephenson, G.; Smith, C. Augmented reality in medical education: Students' experiences and learning outcomes. Med. Educ. Online 2021, 26, 1953953.
69. Park, M.J.; Jung, J.I.; Choi, Y.-S.; Ann, S.H.; Youn, H.-J.; Jeon, G.N.; Choi, H.C. Coronary CT angiography in patients with high calcium score: Evaluation of plaque characteristics and diagnostic accuracy. Int. J. Cardiovasc. Imaging 2011, 27, 43–51.
70. Vavere, A.L.; Arbab-Zadeh, A.; Rochitte, C.E.; Dewey, M.; Niinuma, H.; Gottlieb, I.; Clouse, M.E.; Bush, D.E.; Hoe, J.W.; de Roos, A.; et al. Coronary artery stenoses: Accuracy of 64-detector row CT angiography in segments with mild, moderate, or severe calcification—A subanalysis of the CORE-64 trial. Radiology 2011, 261, 100–108.
71. Chen, C.-C.; Chen, C.-C.; Hsieh, I.C.; Liu, Y.-C.; Liu, C.-Y.; Chan, T.; Wen, M.-S.; Wan, Y.-L. The effect of calcium score on the diagnostic accuracy of coronary computed tomography angiography. Int. J. Cardiovasc. Imaging 2011, 27, 37–42.

72. Meng, L.; Cui, L.; Cheng, Y.; Wu, X.; Tang, Y.; Wang, Y.; Xu, F. Effect of heart rate and coronary calcification on the diagnostic accuracy of the dual-source CT coronary angiography in patients with suspected coronary artery disease. Korean J. Radiol. 2009, 10, 347–354.
73. Meijs, M.F.L.; Meijboom, W.B.; Prokop, M.; Mollet, N.R.; van Mieghem, C.A.G.; Doevendans, P.A.; de Feyter, P.J.; Cramer, M.J. Is there a role for CT coronary angiography in patients with symptomatic angina? Effect of coronary calcium score on identification of stenosis. Int. J. Cardiovasc. Imaging 2009, 25, 847–854.
74. Mergen, V.; Eberhard, M.; Manka, R.; Euler, A.; Alkadhi, H. First in-human quantitative plaque characterization with ultra-high resolution coronary photon-counting CT angiography. Front. Cardiovasc. Med. 2022, 9, 981012.
75. Wolf, E.V.; Halfmann, M.C.; Schoepf, U.J.; Zsarnoczay, E.; Fink, N.; Griffith, J.P., III; Aquino, G.J.; Willemink, M.J.; O'Doherty, J.; Hell, M.M. Intra-individual comparison of coronary calcium scoring between photon counting detector-and energy integrating detector-CT: Effects on risk reclassification. Front. Cardiovasc. Med. 2023, 9, 1053398.
76. Soschynski, M.; Hagen, F.; Baumann, S.; Hagar, M.T.; Weiss, J.; Krauss, T.; Schlett, C.L.; von zur Mühlen, C.; Bamberg, F.; Nikolaou, K.; et al. High Temporal Resolution Dual-Source Photon-Counting CT for Coronary Artery Disease: Initial Multicenter Clinical Experience. J. Clin. Med. 2022, 11, 6003.
77. Karsenty, C.; Guitarte, A.; Dulac, Y.; Briot, J.; Hascoet, S.; Vincent, R.; Delepaul, B.; Vignaud, P.; Djeddai, C.; Hadeed, K.; et al. The usefulness of 3D printed heart models for medical student education in congenital heart disease. BMC Med. Educ. 2021, 21, 480.
78. Lim, K.H.A.; Loo, Z.Y.; Goldie, S.J.; Adams, J.W.; McMenamin, P.G. Use of 3D printed models in medical education: A randomized control trial comparing 3D prints versus cadaveric materials for learning external cardiac anatomy. Anat. Sci. Educ. 2016, 9, 213–221.
79. Su, W.; Xiao, Y.; He, S.; Huang, P.; Deng, X. Three-dimensional printing models in congenital heart disease education for medical students: A controlled comparative study. BMC Med. Educ. 2018, 18, 178.
80. Smith, C.F.; Tollemache, N.; Covill, D.; Johnston, M. Take away body parts! An investigation into the use of 3D-printed anatomical models in undergraduate anatomy education. Anat. Sci. Educ. 2018, 11, 44–53.
81. Yi, X.; Ding, C.; Xu, H.; Huang, T.; Kang, D.; Wang, D. Three-Dimensional Printed Models in Anatomy Education of the Ventricular System: A Randomized Controlled Study. World Neurosurg. 2019, 125, e891–e901.
82. Mogali, S.R.; Chandrasekaran, R.; Radzi, S.; Peh, Z.K.; Tan, G.J.S.; Rajalingam, P.; Yeong, W.Y. Investigating the effectiveness of three-dimensionally printed anatomical models compared with

plastinated human specimens in learning cardiac and neck anatomy: A randomized crossover study. Anat. Sci. Educ. 2022, 15, 1007–1017.

83. Arango, S.; Gorbaty, B.; Brigham, J.; Iaizzo, P.A.; Perry, T.E. A role for ultra-high resolution three-dimensional printed human heart models. Echocardiography 2023, 40, 703–710.
84. Valverde, I.; Gomez-Ciriza, G.; Hussain, T.; Suarez-Mejias, C.; Velasco-Forte, M.N.; Byrne, N.; Ordoñez, A.; Gonzalez-Calle, A.; Anderson, D.; Hazekamp, M.G.; et al. Three-dimensional printed models for surgical planning of complex congenital heart defects: An international multicentre study. Eur. J. Cardiothorac. Surg. 2017, 52, 1139–1148.
85. Cen, J.; Liufu, R.; Wen, S.; Qiu, H.; Liu, X.; Chen, X.; Yuan, H.; Huang, M.; Zhuang, J. Three-Dimensional Printing, Virtual Reality and Mixed Reality for Pulmonary Atresia: Early Surgical Outcomes Evaluation. Heart Lung. Circ. 2021, 30, 296–302.
86. Guo, H.C.; Wang, Y.; Dai, J.; Ren, C.W.; Li, J.H.; Lai, Y.Q. Application of 3D printing in the surgical planning of hypertrophic obstructive cardiomyopathy and physician-patient communication: A preliminary study. J. Thorac. Dis. 2018, 10, 867–873.
87. Ryan, J.; Plasencia, J.; Richardson, R.; Velez, D.; Nigro, J.J.; Pophal, S.; Frakes, D. 3D printing for congenital heart disease: A single site's initial three-yearexperience. 3D Print. Med. 2018, 4, 10.
88. Zhao, L.; Zhou, S.; Fan, T.; Li, B.; Liang, W.; Dong, H. Three-dimensional printing enhances preparation for repair of double outlet right ventricular surgery. J. Cardiac. Surg. 2018, 33, 24–27.
89. Ghosh, R.M.; Jolley, M.A.; Mascio, C.E.; Chen, J.M.; Fuller, S.; Rome, J.J.; Silvestro, E.; Whitehead, K.K. Clinical 3D modeling to guide pediatric cardiothoracic surgery and intervention using 3D printed anatomic models, computer aided design and virtual reality. 3D Print. Med. 2022, 8, 11.
90. Hell, M.M.; Achenbach, S.; Yoo, I.S.; Franke, J.; Blachutzik, F.; Roether, J.; Graf, V.; Raaz-Schrauder, D.; Marwan, M.; Schlundt, C. 3D printing for sizing left atrial appendage closure device: Head-to-head comparison with computed tomography and transoesophageal echocardiography. EuroIntervention 2017, 13, 1234–1241.
91. Russo, J.J.; Yuen, T.; Tan, J.; Willson, A.B.; Gurvitch, R. Assessment of Coronary Artery Obstruction Risk during Transcatheter Aortic Valve Replacement Utilising 3D-Printing. Heart Lung Circ. 2022, 31, 1134–1143.
92. Fan, Y.; Yang, F.; Cheung, G.S.-H.; Chan, A.K.-Y.; Wang, D.D.; Lam, Y.-Y.; Chow, M.C.-K.; Leong, M.C.-W.; Kam, K.K.-H.; So, K.C.-Y.; et al. Device Sizing Guided by Echocardiography-Based Three-Dimensional Printing Is Associated with Superior Outcome after Percutaneous Left Atrial Appendage Occlusion. J. Am. Soc. Echocardiogr. 2019, 32, 708–719.e701.

93. Wu, C.-A.; Squelch, A.; Jansen, S.; Sun, Z. Optimization of computed tomography angiography protocols for follow-up type B aortic dissection patients by using 3D printed model. Appl. Sci. 2021, 11, 6844.
94. Xenofontos, P.; Zamani, R.; Akrami, M. The application of 3D printing in preoperative planning for transcatheter aortic valve replacement: A systematic review. Biomed. Eng. Online 2022, 21, 59.
95. Tanaka, Y.; Saito, S.; Sasuga, S.; Takahashi, A.; Aoyama, Y.; Obama, K.; Umezu, M.; Iwasaki, K. Quantitative assessment of paravalvular leakage after transcatheter aortic valve replacement using a patient-specific pulsatile flow model. Int. J. Cardiol. 2018, 258, 313–320.
96. Brunner, B.S.; Thierij, A.; Jakob, A.; Tengler, A.; Grab, M.; Thierfelder, N.; Leuner, C.J.; Haas, N.A.; Hopfner, C. 3D-printed heart models for hands-on training in pediatric cardiology—The future of modern learning and teaching? GMS J. Med. Educ. 2022, 39, Doc23.
97. Li, H.; Qingyao; Bingshen; Shu, M.; Lizhong; Wang, X.; Song, Z. Application of 3D printing technology to left atrial appendage occlusion. Int. J. Cardiol. 2017, 231, 258–263.
98. Conti, M.; Marconi, S.; Muscogiuri, G.; Guglielmo, M.; Baggiano, A.; Italiano, G.; Mancini, M.E.; Auricchio, F.; Andreini, D.; Rabbat, M.G.; et al. Left atrial appendage closure guided by 3D computed tomography printing technology: A case control study. J. Cardiovasc. Comput. Tomogr. 2019, 13, 336–339.
99. Goitein, O.; Fink, N.; Guetta, V.; Beinart, R.; Brodov, Y.; Konen, E.; Goitein, D.; Di Segni, E.; Grupper, A.; Glikson, M. Printed MDCT 3D models for prediction of left atrial appendage (LAA) occluder device size: A feasibility study. EuroIntervention 2017, 13, e1076–e1079.
100. Traynor, G.; Shearn, A.I.; Milano, E.G.; Ordonez, M.V.; Forte, M.N.V.; Caputo, M.; Schievano, S.; Mustard, H.; Wray, J.; Biglino, G. The use of 3D-printed models in patient communication: A scoping review. J. 3D Print. Med. 2022, 6, 13–23.
101. Illmann, C.F.; Hosking, M.; Harris, K.C. Utility and Access to 3-Dimensional Printing in the Context of Congenital Heart Disease: An International Physician Survey Study. CJC Open. 2020, 2, 207–213.
102. Biglino, G.; Capelli, C.; Leaver, L.-K.; Schievano, S.; Taylor, A.M.; Wray, J. Involving patients, families and medical staff in the evaluation of 3D printing models of congenital heart disease. Commun. Med. 2015, 12, 157–169.
103. Lau, I.W.W.; Liu, D.; Xu, L.; Fan, Z.; Sun, Z. Clinical value of patient-specific three-dimensional printing of congenital heart disease: Quantitative and qualitative assessments. PLoS ONE 2018, 13, e0194333.
104. Biglino, G.; Koniordou, D.; Gasparini, M.; Capelli, C.; Leaver, L.-K.; Khambadkone, S.; Schievano, S.; Taylor, A.M.; Wray, J. Piloting the Use of Patient-Specific Cardiac Models as a Novel Tool to Facilitate Communication During Cinical Consultations. Pediatr. Cardiol. 2017, 38, 813–818.

105. Giovanni, B.; Claudio, C.; Jo, W.; Silvia, S.; Lindsay-Kay, L.; Sachin, K.; Alessandro, G.; Graham, D.; Alexander, J.; Andrew, M.T. 3D-manufactured patient-specific models of congenital heart defects for communication in clinical practice: Feasibility and acceptability. BMJ Open 2015, 5, e007165.

106. Biglino, G.; Moharem-Elgamal, S.; Lee, M.; Tulloh, R.; Caputo, M. The Perception of a Three-Dimensional-Printed Heart Model from the Perspective of Different Stakeholders: A Complex Case of Truncus Arteriosus. Front. Pediatr. 2017, 5, 209.

107. Wu, C.-A.; Squelch, A.; Sun, Z. Investigation of Three-dimensional Printing Materials for Printing Aorta Model Replicating Type B Aortic Dissection. Curr. Med. Imaging Rev. 2021, 17, 843–849.

108. Sun, Z.; Ng, C.K.C.; Wong, Y.H.; Yeong, C.H. 3D-Printed Coronary Plaques to Simulate High Calcification in the Coronary Arteries for Investigation of Blooming Artifacts. Biomolecules 2021, 11, 1307.

109. Sun, Z.; Ng, C.K.C.; Squelch, A. Synchrotron radiation computed tomography assessment of calcified plaques and coronary stenosis with different slice thicknesses and beam energies on 3D printed coronary models. Quant. Imaging Med. Surg. 2019, 9, 6–22.

110. Sun, Z. 3D printed coronary models offer new opportunities for developing optimal coronary CT angiography protocols in imaging coronary stents. Quant. Imaging Med. Surg. 2019, 9, 1350–1355.

111. Sun, Z. 3D printing in medical applications. Curr. Med. Imaging. 2021, 17, 811–813.

112. Sommer, K.N.; Iyer, V.; Kumamaru, K.K.; Rava, R.A.; Ionita, C.N. Method to simulate distal flow resistance in coronary arteries in 3D printed patient specific coronary models. 3D Print. Med. 2020, 6, 19.

113. Wu, C.-A.; Squelch, A.; Sun, Z. Assessment of optimization of computed tomography angiography protocols for follow-up type B aortic dissection patients by using a 3D-printed model. J. 3D Print. Med. 2022, 6, 117–127.

114. Aldosari, S.; Jansen, S.; Sun, Z. Optimization of computed tomography pulmonary angiography protocols using 3D printed model with simulation of pulmonary embolism. Quant. Imaging Med. Surg. 2019, 9, 53–62.

115. Aldosari, S.; Jansen, S.; Sun, Z. Patient-specific 3D printed pulmonary artery model with simulation of peripheral pulmonary embolism for developing optimal computed tomography pulmonary angiography protocols. Quant. Imaging Med. Surg. 2019, 9, 75–85.

116. Sun, Z.; Jansen, S. Personalized 3D printed coronary models in coronary stenting. Quant. Imaging Med. Surg. 2019, 9, 1356–1367.

117. Ripley, B.; Kelil, T.; Cheezum, M.K.; Goncalves, A.; Di Carli, M.F.; Rybicki, F.J.; Steigner, M.; Mitsouras, D.; Blankstein, R. 3D printing based on cardiac CT assists anatomic visualization prior to transcatheter aortic valve replacement. J. Cardiovasc. Comput. Tomogr. 2016, 10, 28–36.

118. Kiraly, L.; Shah, N.C.; Abdullah, O.; Al-Ketan, O.; Rowshan, R. Three-Dimensional Virtual and Printed Prototypes in Complex Congenital and Pediatric Cardiac Surgery—A Multidisciplinary Team-Learning Experience. Biomolecules 2021, 11, 1703.

119. Ullah, M.; Bibi, A.; Wahab, A.; Hamayun, S.; Rehman, M.U.; Khan, S.U.; Awan, U.A.; Riaz, N.-u.-a.; Naeem, M.; Saeed, S.; et al. Shaping the Future of Cardiovascular Disease by 3D Printing Applications in Stent Technology and its Clinical Outcomes. Curr. Probl. Cardiol. 2024, 49, 102039.

120. Sun, Z.; Zhao, J.; Leung, E.; Flandes-Iparraguirre, M.; Vernon, M.; Silberstein, J.; De-Juan-Pardo, E.M.; Jansen, S. Three-Dimensional Bioprinting in Cardiovascular Disease: Current Status and Future Directions. Biomolecules 2023, 13, 1180.

121. Jana, S.; Tefft, B.J.; Spoon, D.B.; Simari, R.D. Scaffolds for tissue engineering of cardiac valves. Acta Biomater. 2014, 10, 2877–2893.

122. Mela, P. Subject- and Leaflet-Specific Remodeling of Polymeric Heart Valves for In Situ Tissue Engineering. JACC Basic. Transl. Sci. 2020, 5, 32–34.

123. Vesely, I. Heart Valve Tissue Engineering. Circ. Res. 2005, 97, 743–755.

124. Wissing, T.B.; Bonito, V.; Bouten, C.V.C.; Smits, A.I.P.M. Biomaterial-driven in situ cardiovascular tissue engineering—A multi-disciplinary perspective. npj Regen. Med. 2017, 2, 18.

125. Butcher, J.T. The root problem of heart valve engineering. Sci. Transl. Med. 2018, 10, eaat5850.

126. Tomasina, C.; Bodet, T.; Mota, C.; Moroni, L.; Camarero-Espinosa, S. Bioprinting Vasculature: Materials, Cells and Emergent Techniques. Materials 2019, 12, 2701.

127. Seymour, A.J.; Westerfield, A.D.; Cornelius, V.C.; Skylar-Scott, M.A.; Heilshorn, S.C. Bioprinted microvasculature: Progressing from structure to function. Biofabrication 2022, 14, 22002.

128. Wang, Z.; Wang, L.; Li, T.; Liu, S.; Guo, B.; Huang, W.; Wu, Y. 3D bioprinting in cardiac tissue engineering. Theranostics 2021, 11, 7948–7969.

129. Bejleri, D.; Streeter, B.W.; Nachlas, A.L.Y.; Brown, M.E.; Gaetani, R.; Christman, K.L.; Davis, M.E. A Bioprinted Cardiac Patch Composed of Cardiac-Specific Extracellular Matrix and Progenitor Cells for Heart Repair. Adv. Healthc. Mater. 2018, 7, e1800672.

130. Zhu, K.; Shin, S.R.; van Kempen, T.; Li, Y.C.; Ponraj, V.; Nasajpour, A.; Mandla, S.; Hu, N.; Liu, X.; Leijten, J.; et al. Tissue Engineering: Gold Nanocomposite Bioink for Printing 3D Cardiac Constructs. Adv. Funct. Mater. 2017, 27, 1605352.

131. Erdem, A.; Darabi, M.A.; Nasiri, R.; Sangabathuni, S.; Ertas, Y.N.; Alem, H.; Hosseini, V.; Shamloo, A.; Nasr, A.S.; Ahadian, S.; et al. 3D Bioprinting of Oxygenated Cell-Laden Gelatin Methacryloyl Constructs. Adv. Healthc. Mater. 2020, 9, e1901794.

132. Ahrens, J.H.; Uzel, S.G.M.; Skylar-Scott, M.; Mata, M.M.; Lu, A.; Kroll, K.T.; Lewis, J.A. Programming Cellular Alignment in Engineered Cardiac Tissue via Bioprinting Anisotropic Organ Building Blocks. Adv. Mater. 2022, 34, e2200217.

133. Asulin, M.; Michael, I.; Shapira, A.; Dvir, T. One-Step 3D Printing of Heart Patches with Built-in Electronics for Performance Regulation. Adv. Sci. 2021, 8, 2004205.

134. Häneke, T.; Sahara, M. Progress in Bioengineering Strategies for Heart Regenerative Medicine. Int. J. Mol. Sci. 2022, 23, 3482.

135. Zhou, Z.; Tang, W.; Yang, J.; Fan, C. Application of 4D printing and bioprinting in cardiovascular tissue engineering. Biomater. Sci. 2023, 11, 6403–6420.

136. Pijls, N.H.J.; Van Schaardenburgh, P.; De Bruyne, B.; Manoharan, G.; Boersma, E.; Bech, J.-W.; Vant Veer, M.; BÄR, F.; Hoorntje, J.; Koolen, J.; et al. Percutaneous coronary intervention of functionally nonsignificant stenosis: 5-year follow-up of the DEFER Study. J. Am. Coll. Cardiol. 2007, 49, 2105–2111.

137. Zimmermann, F.M.; Ferrara, A.; Johnson, N.P.; van Nunen, L.X.; Escaned, J.; Albertsson, P.; Erbel, R.; Legrand, V.; Gwon, H.-C.; Remkes, W.S.; et al. Deferral vs. performance of percutaneous coronary intervention of functionally non-significant coronary stenosis: 15-year follow-up of the DEFER trial. Eur. Heart J. 2015, 36, 3182–3188.

138. Tonino, P.A.L.; De Bruyne, B.; Pijls, N.H.J.; Siebert, U.; Ikeno, F.; van't Veer, M.; Klauss, V.; Manoharan, G.; Engstrøm, T.; Oldroyd, K.G.; et al. Fractional Flow Reserve versus Angiography for Guiding Percutaneous Coronary Intervention. N. Eng. J. Med. 2009, 360, 213–224.

139. Pijls, N.H.J.; Fearon, W.F.; Oldroyd, K.G.; Ver Lee, P.N.; Maccarthy, P.A.; De Bruyne, B.; Tonino, P.A.L.; Siebert, U.; Ikeno, F.; Bornschein, B.; et al. Fractional Flow Reserve Versus Angiography for Guiding Percutaneous Coronary Intervention in Patients with Multivessel Coronary Artery Disease: 2-Year Follow-up of the FAME (Fractional Flow Reserve Versus Angiography for Multivessel Evaluation) Study. J. Am. Coll. Cardiol. 2010, 56, 177–184.

140. Van Nunen, L.X.M.D.; Zimmermann, F.M.M.D.; Tonino, P.A.L.P.; Barbato, E.P.; Baumbach, A.P.; Engstrøm, T.P.; Klauss, V.P.; MacCarthy, P.A.P.; Manoharan, G.M.D.; Oldroyd, K.G.P.; et al. Fractional flow reserve versus angiography for guidance of PCI in patients with multivessel coronary artery disease (FAME): 5-year follow-up of a randomised controlled trial. Lancet 2015, 386, 1853–1860.

141. Fearon, W.F.; Tonino, P.A.; De Bruyne, B.; Siebert, U.; Pijls, N.H. Rationale and design of the fractional flow reserve versus angiography for multivessel evaluation (FAME) study. Am. Heart J.

2007, 154, 632–636.

142. Fearon, W.F.; Bornschein, B.; Tonino, P.A.L.; Gothe, R.M.; De Bruyne, B.; Pijls, N.H.J.; Siebert, U. Economic Evaluation of Fractional Flow Reserve-Guided Percutaneous Coronary Intervention in Patients With Multivessel Disease. Circulation 2010, 122, 2545–2550.
143. De Bruyne, B.; Pijls, N.H.J.; Kalesan, B.; Barbato, E.; Tonino, P.A.L.; Piroth, Z.; Jagic, N.; Mobius-Winckler, S.; Rioufol, G.; Witt, N.; et al. Fractional Flow Reserve–Guided PCI versus Medical Therapy in Stable Coronary Disease. N. Eng. J. Med. 2012, 367, 991–1001.
144. Jung, C.; Wolff, G.; Wernly, B.; Bruno, R.R.; Franz, M.; Schulze, P.C.; Silva, J.N.A.; Silva, J.R.; Bhatt, D.L.; Kelm, M. Virtual and Augmented Reality in Cardiovascular Care: State-of-the-Art and Future Perspectives. JACC Cardiovasc. Imaging 2022, 15, 519–532.
145. Mitsuno, D.; Ueda, K.; Hirota, Y.; Ogino, M. Effective Application of Mixed Reality Device HoloLens: Simple Manual Alignment of Surgical Field and Holograms. Plast. Reconstr. Surg. 2019, 143, 647–651.
146. Moro, C.; Phelps, C.; Redmond, P.; Stromberga, Z. HoloLens and mobile augmented reality in medical and health science education: A randomised controlled trial. Br. J. Educ. Technol. 2021, 52, 680–694.
147. Gehrsitz, P.; Rompel, O.; Schöber, M.; Cesnjevar, R.; Purbojo, A.; Uder, M.; Dittrich, S.; Alkassar, M. Cinematic Rendering in Mixed-Reality Holograms: A New 3D Preoperative Planning Tool in Pediatric Heart Surgery. Front. Cardiovasc. Med. 2021, 8, 633611.
148. Soulami, R.B.; Verhoye, J.-P.; Duc, H.N.; Castro, M.; Auffret, V.; Anselmi, A.; Haigron, P.; Ruggieri, V.G. Computer-Assisted Transcatheter Heart Valve Implantation in Valve-in-Valve Procedures. Innovations 2016, 11, 193–200.
149. Opolski, M.P.; Debski, A.; Borucki, B.A.; Staruch, A.D.; Kepka, C.; Rokicki, J.K.; Sieradzki, B.; Witkowski, A. Feasibility and safety of augmented-reality glass for computed tomography-assisted percutaneous revascularization of coronary chronic total occlusion: A single center prospective pilot study. J. Cardiovasc. Comput. Tomogr. 2017, 11, 489–496.
150. Ye, W.; Zhang, X.; Li, T.; Luo, C.; Yang, L. Mixed-reality hologram for diagnosis and surgical planning of double outlet of the right ventricle: A pilot study. Clin. Radiol. 2021, 76, 237.e1–237.e7.
151. Kumar, R.P.; Pelanis, E.; Bugge, R.; Brun, H.; Palomar, R.; Aghayan, D.L.; Fretland, Å.A.; Edwin, B.; Elle, O.J. Use of mixed reality for surgery planning: Assessment and development workflow. J. Biomed. Inform. 2020, 112, 100077.
152. Brun, H.; Bugge, R.A.B.; Suther, L.K.R.; Birkeland, S.; Kumar, R.; Pelanis, E.; Elle, O.J. Mixed reality holograms for heart surgery planning: First user experience in congenital heart disease. Eur. Heart J. Cardiovasc. Imaging 2019, 20, 883–888.

153. Lau, I.; Gupta, A.; Sun, Z. Clinical Value of Virtual Reality versus 3D Printing in Congenital Heart Disease. Biomolecules 2021, 11, 884.

154. Yang, J.; Shan, D.; Wang, X.; Sun, X.; Shao, M.; Wang, K.; Pan, Y.; Wang, Z.; Schoepf, U.J.; Savage, R.H.; et al. On-Site Computed Tomography-Derived Fractional Flow Reserve to Guide Management of Patients with Stable Coronary Artery Disease: The TARGET Randomized Trial. Circulation 2023, 147, 1369–1381.

155. Wang, H.; Wang, R.; Li, Y.; Zhou, Z.; Gao, Y.; Bo, K.; Yu, M.; Sun, Z.; Xu, L. Assessment of Image Quality of Coronary Computed Tomography Angiography in Obese Patients by Comparing Deep Learning Image Reconstruction with Adaptive Statistical Iterative Reconstruction Veo. J. Comput. Assist. Tomogr. 2022, 46, 34–40.

156. Wang, W.; Wang, H.; Chen, Q.; Zhou, Z.; Wang, R.; Wang, H.; Zhang, N.; Chen, Y.; Sun, Z.; Xu, L. Coronary artery calcium score quantification using a deep-learning algorithm. Clin. Radiol. 2020, 75, e211–e237.

157. Han, D.; Liu, J.; Sun, Z.; Cui, Y.; He, Y.; Yang, Z. Deep learning analysis in coronary computed tomographic angiography imaging for the assessment of patients with coronary artery stenosis. Comput. Methods Programs. Biomed. 2020, 196, 105651.

158. Gao, Y.; Wang, W.; Wang, H.; Zhou, Z.; Xu, P.; Jiang, M.; Yang, L.; Wang, H.; Wen, H.; Sun, Z.; et al. Impact of Sublingual Nitroglycerin on the Assessment of Computed Tomography–derived Fractional Flow Reserve: An Intraindividual Comparison Study. J. Comput. Assist. Tomogr. 2022, 46, 23–28.

159. Sun, Z.; Ng, C.K. Artificial intelligence (enhanced super-resolution generative adversarial network) for calcium deblooming in coronary computed tomography angiography: A feasibility study. Diagnostics 2022, 12, 991.

160. Sun, Z.; Ng, C.K. Finetuned super-resolution generative adversarial network (artificial intelligence) model for calcium deblooming in coronary computed tomography angiography. J. Pers. Med. 2022, 12, 1354.

161. Li, P.; Xu, L.; Yang, L.; Wang, R.; Hsieh, J.; Sun, Z.; Fan, Z.; Leipsic, J.A. Blooming Artifact Reduction in Coronary Artery Calcification by a New De-blooming Algorithm: Initial Study. Sci. Rep. 2018, 8, 6945.

162. Alskaf, E.; Dutta, U.; Scannell, C.M.; Chiribiri, A. Deep learning applications in coronary anatomy imaging: A systematic review and meta-analysis. J. Med. Artif. Intell. 2022, 5, 11.

163. Lin, A.; Manral, N.; McElhinney, P.; Killekar, A.; Matsumoto, H.; Kwiecinski, J.; Pieszko, K.; Razipour, A.; Grodecki, K.; Park, C.; et al. Deep learning-enabled coronary CT angiography for plaque and stenosis quantification and cardiac risk prediction: An international multicentre study. Lancet 2022, 4, e256–e265.

164. Raffort, J.; Adam, C.; Carrier, M.; Ballaith, A.; Coscas, R.; Jean-Baptiste, E.; Hassen-Khodja, R.; Chakfé, N.; Lareyre, F. Artificial intelligence in abdominal aortic aneurysm. J. Vasc. Surg. 2020, 72, 321–333.e321.

165. Lareyre, F.; Adam, C.; Carrier, M.; Dommerc, C.; Mialhe, C.; Raffort, J. A fully automated pipeline for mining abdominal aortic aneurysm using image segmentation. Sci. Rep. 2019, 9, 13750.

166. Spinella, G.; Fantazzini, A.; Finotello, A.; Vincenzi, E.; Boschetti, G.A.; Brutti, F.; Magliocco, M.; Pane, B.; Basso, C.; Conti, M. Artificial Intelligence Application to Screen Abdominal Aortic Aneurysm Using Computed tomography Angiography. J. Digit. Imaging 2023, 36, 2125–2137.

167. Chandra, S.; Sarkar, P.K.; Chandra, D.; Ginsberg, N.E.; Cohen, R.I. Finding an alternative diagnosis does not justify increased use of CT-pulmonary angiography. BMC Pulm. Med. 2013, 13, 9.

168. Soffer, S.; Klang, E.; Shimon, O.; Barash, Y.; Cahan, N.; Greenspana, H.; Konen, E. Deep learning for pulmonary embolism detection on computed tomography pulmonary angiogram: A systematic review and meta-analysis. Sci. Rep. 2021, 11, 15814.

169. Huhtanen, H.; Nyman, M.; Mohsen, T.; Virkki, A.; Karlsson, A.; Hirvonen, J. Automated detection of pulmonary embolism from CT-angiograms using deep learning. BMC Med. Imaging 2022, 22, 43.

170. Ma, X.; Ferguson, E.C.; Jiang, X.; Savitz, S.I.; Shams, S. A multitask deep learning approach for pulmonary embolism detection and identification. Sci. Rep. 2022, 12, 13087.

171. Grenier, P.A.; Ayobi, A.; Quenet, S.; Tassy, M.; Marx, M.; Chow, D.S.; Weinberg, B.D.; Chang, P.D.; Chaibi, Y. Deep Learning-Based Algorithm for Automatic Detection of Pulmonary Embolism in Chest CT Angiograms. Diagnostics 2023, 13, 1324.

172. Colak, E.; Kitamura, F.C.; Hobbs, S.B.; Wu, C.C.; Lungren, M.P.; Prevedello, L.M.; Kalpathy-Cramer, J.; Ball, R.L.; Shih, G.; Stein, A.; et al. The RSNA Pulmonary Embolism CT Dataset. Radiol. Artif. Intell. 2021, 3, e200254.

173. Jiang, B.; Guo, N.; Ge, Y.; Zhang, L.; Oudkerk, M.; Xie, X. Development and application of artificial intelligence in cardiac imaging. Br. J. Radiol. 2020, 93, 20190812.